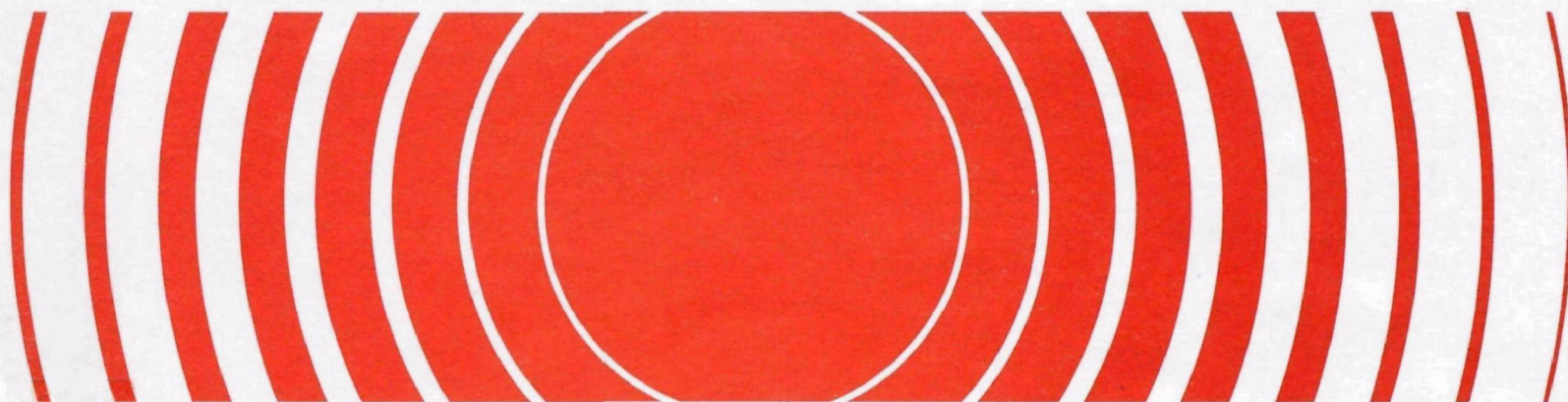




# **Analysis And Evaluation Of A Radioactive Waste Package Retrieved From The Farallon Islands 900-Meter Disposal Site**



**ANALYSIS AND EVALUATION  
OF A RADIOACTIVE WASTE PACKAGE  
RETRIEVED FROM  
THE FARALLON ISLANDS 900-METER DISPOSAL SITE**

**September 1990**

**by**

**P. Colombo and M. W. Kendig  
Waste Management R&D Group  
Department of Nuclear Energy  
Brookhaven National Laboratory  
Associated Universities, Inc.  
Upton, New York 11973**

**This study was conducted for the  
U.S. Environmental Protection Agency  
under Interagency Agreement No. EPA-IAG-D6-0166**

**PROJECT OFFICER  
Robert S. Dyer  
Office of Radiation Programs  
U.S. Environmental Protection Agency  
Washington, DC 20460**

## FOREWORD

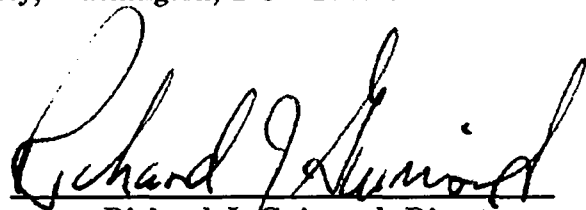
The Environmental Protection Agency (EPA) was given a Congressional mandate to develop criteria and regulations governing the ocean disposal of all forms of waste, pursuant to Public Law 92-532 (the Marine Protection, Research and Sanctuaries Act of 1972) and, as amended, by Public Law 97-424. The EPA has taken an active role, nationally and within the international nuclear regulatory community, to develop the effective controls needed to protect the health and safety of man and to safeguard the marine environment.

In 1974 the EPA Office of Radiation Programs (ORP) first initiated feasibility studies to determine whether existing technologies could be applied toward assessing the fate of radioactive wastes that had previously been disposed in the oceans. After successfully locating waste packages in ocean sites formerly used by the U.S. to dispose of radioactive waste materials, ORP developed a program of site characterization studies to determine the biological, chemical, geological and physical characteristics of the marine environment, in and near the disposal sites. These studies also included evaluations of the concentration and distribution of radionuclides within and near the disposal sites.

In addition, ORP has retrieved radioactive waste containers from three deep-ocean disposal sites to evaluate the performance, with time, of past packaging techniques. Under an interagency agreement with ORP, the Brookhaven National Laboratory (BNL) has performed container corrosion and matrix analysis studies on the recovered radioactive waste packages. The results of BNL's first analysis of a LLW package recovered, in 1976, from the deep-ocean were published in EPA Technical Report No. EPA 520/1-82-009, "Analysis and Evaluation of a Recovered Radioactive Waste Package from the Atlantic 2800 Meter Disposal Site."

In 1977, ORP recovered another LLW package from the Farallon Islands 900-meter disposal site. This report details the BNL analysis of that waste package.

Readers of this report are invited to send comments or suggestions to Mr. Martin P. Halper, Director, Analysis and Support Division (ANR-461), Office of Radiation Programs, U.S. Environmental Protection Agency, Washington, DC 20460.

A handwritten signature in black ink, reading "Richard J. Guimond". The signature is fluid and cursive, with the first name "Richard" being the most prominent part.

Richard J. Guimond, Director  
Office of Radiation Programs

## Table of Contents

<b>FOREWORD</b>	<b>iii</b>
<b>List of Figures</b>	<b>vii</b>
<b>List of Tables</b>	<b>ix</b>
<b>1. INTRODUCTION</b>	<b>1</b>
<b>1.1. FARALLON ISLANDS RADIOACTIVE             WASTE DISPOSAL SITE</b>	<b>1</b>
<b>1.2 WASTE INVENTORY</b>	<b>1</b>
<b>1.3 WASTE TYPES</b>	<b>4</b>
<b>1.4 WASTE PACKAGING TECHNIQUES</b>	<b>4</b>
<b>2. SURVEY AND RECOVERY OF A WASTE PACKAGE FROM THE 900-METER SITE</b>	<b>6</b>
<b>2.1 FARALLON ISLANDS 900-METER DISPOSAL             SITE SURVEY (1974)</b>	<b>6</b>
<b>2.2 RETRIEVAL OF A WASTE PACKAGE FROM THE             FARALLON ISLANDS 900-METER SUBSITE</b>	<b>8</b>
<b>2.2.1 <u>Retrieval Operation</u></b>	<b>8</b>
<b>2.2.2 <u>Radiation Surveillance</u></b>	<b>15</b>
<b>2.2.3 <u>Shipboard Inspection</u></b>	<b>19</b>
<b>2.2.4 <u>Storage and Transportation</u></b>	<b>21</b>
<b>3. ANALYSIS OF THE CONCRETE WASTE FORM</b>	<b>22</b>
<b>3.1 RADIOGRAPHY</b>	<b>22</b>
<b>3.2 CONTAINER REMOVAL</b>	<b>25</b>
<b>3.3 CONCRETE CORING</b>	<b>25</b>
<b>3.4 WASTE CONTENT</b>	<b>27</b>
<b>3.5 RADIOACTIVITY</b>	<b>30</b>
<b>3.6 WASTE FORM INTEGRITY</b>	<b>30</b>
<b>4. CORROSION ANALYSIS OF THE METAL CONTAINER</b>	<b>33</b>
<b>4.1 VISUAL INSPECTION AND SAMPLING</b>	<b>33</b>
<b>4.2 DIMENSIONAL ANALYSIS</b>	<b>34</b>
<b>4.3 PROTECTED REGION ON THE SEDIMENT SIDE</b>	<b>46</b>
<b>4.4 CORRODED REGION ON THE SEA SIDE</b>	<b>50</b>
<b>5. CONCLUSIONS</b>	<b>63</b>
<b>REFERENCES</b>	<b>64</b>



## List of Figures

Figure 1.1	Farallon Islands Radioactive Waste Disposal Sites . . . . .	2
Figure 1.2	Cut Away Isometric Views Showing Modifications of 55-Gallon Drums for Packaging Radioactive Wastes Which Were Disposed of In The Farallon Islands Disposal Site . . . . .	5
Figure 2.1	Unmanned Cable Controlled Underwater Recovery Vehicle, CURV III . . . . .	7
Figure 2.2	Manned Submersible PISCES VI . . . . .	9
Figure 2.3	Canadian Research Vessel PANDORA II . . . . .	10
Figure 2.4	University of Southern California Research Vessel VELERO IV	10
Figure 2.5	Waste Package Showing Severe Hydrostatic Implosion . . . . .	12
Figure 2.6	Waste Package Showing Mild Hydrostatic Implosion . . . . .	12
Figure 2.7	Waste Package Showing No Signs of Hydrostatic Implosion . . . . .	13
Figure 2.8	Underwater Inspection of Recovered Waste Package . . . . .	14
Figure 2.9	View of the Wire Rope Lifting Eye Imbedded into the Concrete Waste Form . . . . .	14
Figure 2.10	Submersible PISCES VI Being Launched For Waste Package Recovery . . . . .	16
Figure 2.11	Waste Package Being Hoisted Aboard the Research Vessel VELERO IV . . . . .	18
Figure 2.12	The Waste Package Being Prepared for Visual Inspection . . . . .	18
Figure 2.13	A View of the Corrosion on the Sea Side of the Container . . . . .	20
Figure 2.14	Sea Worms Attached to the Concrete Surface of the Waste Form	20
Figure 3.1	Removal of the Waste Package From the Shipping Container . . . . .	23
Figure 3.2	View of the Sediment Side of the Waste Container . . . . .	24
Figure 3.3	Concrete Waste Form After Removal of Container . . . . .	26
Figure 3.4	View of the Position of the Cardboard Box Embedded in Cement	28
Figure 3.5	Closeup of Parted Waste Form . . . . .	29
Figure 3.6	Legibility of Printed Matter on Cardboard Box . . . . .	29

### List of Figures (Continued)

Figure 4.1	Schematic of Coordinate System Used to Identify Locations on the Container . . . . .	35
Figure 4.2	View of Waste Package Showing the Sediment Side ( $0^{\circ}$ - $90^{\circ}$ )	36
Figure 4.3	View of Waste Package Showing . . . . .	37
Figure 4.4	View of Waste Package Showing the Sea Side ( $180^{\circ}$ - $270^{\circ}$ ) .	38
Figure 4.5	View of Waste Package Showing the Sea Side ( $270^{\circ}$ - $360^{\circ}$ ) .	39
Figure 4.6	Nodule of Corrosion Product on Sea Side . . . . .	40
Figure 4.7	Strips Extracted for Metal Loss Analysis . . . . .	41
Figure 4.8	Perforations Observed Prior to Cutting Sheath . . . . .	42
Figure 4.9	View of the Sheath from the Concrete Side . . . . .	43
Figure 4.10	Closeup of a Chime Perforation . . . . .	44
Figure 4.11	Metal Thickness as a Function of Position . . . . .	48
Figure 4.12	Optical Micrograph of Well Protected Specimens Taken from Positions ( $x = 9$ inches, $\theta = 45^{\circ}$ ), ( $x = 15$ inches, $\theta = 45^{\circ}$ ) respectively . . . . .	51
Figure 4.13	Initiation of Corrosion on the Sediment Side of the Container ( $x=12$ inches, $\theta = 46^{\circ}$ ) . . . . .	52
Figure 4.14	Rapid General Corrosion on Sample Taken from $X=27$ inches, $\theta = 225^{\circ}$ . . . . .	53
Figure 4.15	Metal to Scale Interface of Sample Taken From $x=27$ inches, $\theta = 225^{\circ}$ . . . . .	54
Figure 4.16	Corrosion Scale of Sample (Concrete Side) Taken From $x=27$ inches, $\theta = 225^{\circ}$ . . . . .	55
Figure 4.17	Solid Phase Analysis of Concrete Side Lamina of Sample Taken from $x=27$ inches, $\theta = 225^{\circ}$ . . . . .	56
Figure 4.18	Schematic of Container with Scale Growth . . . . .	57

List of Tables

TABLE 1.1	<u>FARALLON ISLANDS RADIOACTIVE WASTE DISPOSAL SITE</u> . . . . .	3
TABLE 3.1	<u>COMPRESSIVE STRENGTH OF CONCRETE CORES</u> . . . . .	32
TABLE 4.1	<u>SCRAPINGS</u> . . . . .	45
TABLE 4.2	<u>CALCULATED CORROSION RATES</u> . . . . .	49
TABLE 4.3	<u>TRACE ELEMENT ANALYSES OF CONTAINER MATERIAL</u> . . . . .	60
TABLE 4.4	<u>X-RAY FLUORESCENCE ANALYSIS OF TRACE COMPONENTS IN SCRAPINGS</u>	61
TABLE 4.5	<u>X-RAY DIFFRACTION ANALYSIS OF MAJOR IRON OXIDE COMPONENT</u> .	62

## 1. INTRODUCTION

### 1.1 FARALLON ISLANDS RADIOACTIVE WASTE DISPOSAL SITE

Between 1946 and 1970, the United States disposed of radioactive wastes by ocean disposal at designated sites licensed by the Atomic Energy Commission (AEC).

An ocean area near the Farallon Islands was one of the sites designated by the AEC for ocean disposal of radioactive wastes. This site received the majority of all wastes deposited in the Pacific Ocean.

The Farallons are a chain of uninhabited islands extending in a northwest direction approximately 70 kilometers (40 miles) west of San Francisco, California. The site actually consists of three separate subsites, identified as 1, 2 and 3, in Figure 1.1. Each subsite was officially used for varying periods of time between 1946-1965.

The first area selected for receiving radioactive waste packages in 1946 was subsite 1, having a depth of approximately 92 meters. During the latter part of 1946, the disposal operations were transferred to subsite 3 which is located 77 kilometers (45 miles) from land at a depth of 1700 meters. Disposal operations continued at this site until 1951 when subsite 2, at a depth of 900 meters, was designated as the only subsite for disposal of radioactive wastes. The reason for this new subsite designation is not entirely clear although it may be attributed to the fact that subsite 3 was also used to dispose of chemical munitions. The greater distance from land may also have been a consideration. In 1954, however, disposal was resumed at subsite 3 and it continued until 1965 when land disposal sites were licensed to receive radioactive waste [1].

### 1.2 WASTE INVENTORY

Table 1.1 gives the estimated number of waste packages and total activity deposited at the three Farallon Islands subsites. During the time period when ocean disposal was in effect, detailed recordkeeping was generally not required since the disposal of radioactive waste was considered a "garbage disposal type of operation" [2]. Consequently, a complete assessment cannot be made of the total number of packages or curies of radioactivity of the packages which were disposed of at the Pacific Ocean radioactive disposal sites.

Most of the wastes disposed at the Farallon Islands site were generated by: (1) the U.S. Naval Radiological Defense Laboratory, (2) the University of California Lawrence Livermore Radiation Laboratory, and (3) the University of California Radiation Laboratory at Berkeley. The radioactive waste disposal operations were conducted by the U.S. Navy until July 1959 when private companies assumed the responsibility under AEC license.

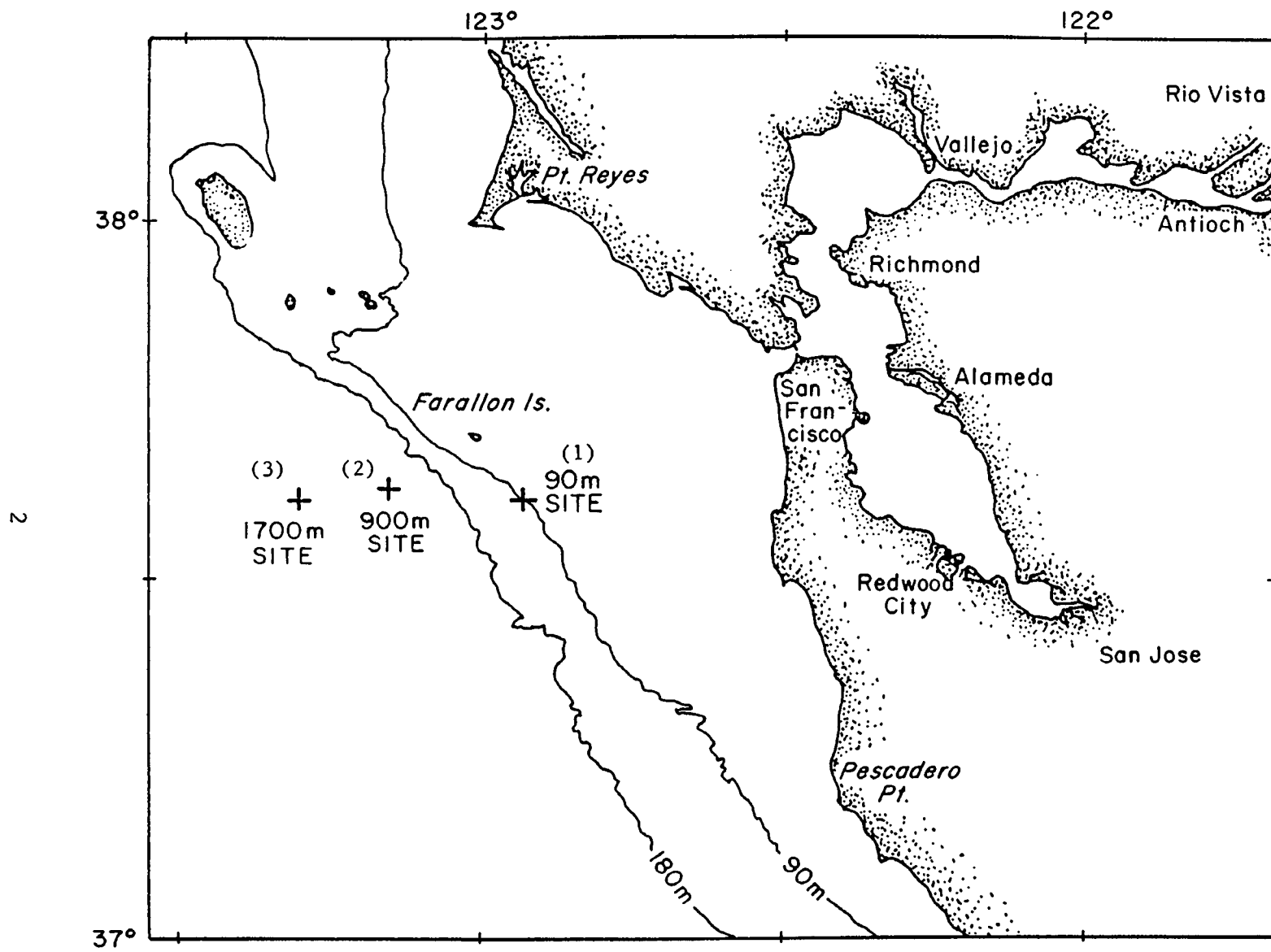


Figure 1.1 Farallon Islands Radioactive Waste Disposal Sites



TABLE 1.1

FARALLON ISLANDS RADIOACTIVE WASTE DISPOSAL SITE

<u>Subsite</u>	<u>Coordinates</u>	<u>Depth (m)</u>	<u>Distance From Land (km)</u>	<u>Years Used</u>	<u>Estimated No. of 55-Gallon Waste Packages</u>	<u>Estimated Activity (Ci)</u>
1	37° 38'N 122° 58'W	90 (300 ft)	45 (28 miles)	1946	150	unknown
2	37° 38'N 123° 08'W	900 (3000 ft)	60 (40 miles)	1951-1953	3,600	1,100
3	37° 37'N 123° 17'W	1700 (5300 ft)	77 (50 miles)	1946-1950 1954-1964	44,000	13,400

### 1.3 WASTE TYPES

Both defense waste and waste generated at commercial and medical facilities consisted of materials having activity levels normally associated with laboratory operations. The waste inventories represented an extremely heterogeneous group of liquid and solid materials with physical and chemical properties varying over a great compositional range. Typical solid waste consisted of contaminated paper, metals, rubber, rags, and glass. The wet waste included filter cartridges, aqueous solutions, evaporator concentrates, solvents and other miscellaneous materials.

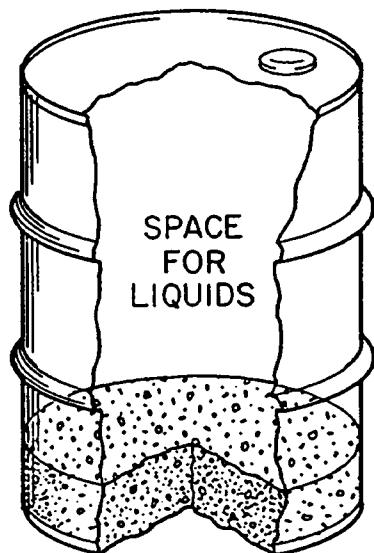
In general, radiation contamination was mainly by beta-gamma emitters evolving from reactor experimental materials and byproducts of isotope production having half-lives greater than one year. Many of the early waste packages disposed in the Farallon Islands site contained alpha-emitting wastes generated by particle accelerators. It is estimated that approximately 30 curies of alpha activity was packaged and disposed through 1953 [2].

### 1.4 WASTE PACKAGING TECHNIQUES

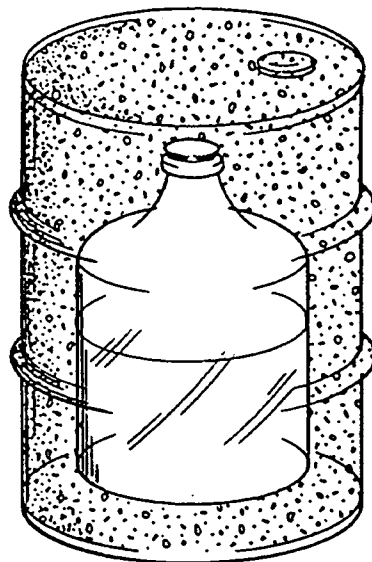
Most of the waste disposed at the Farallon Islands site was packaged in used or reconditioned 55-gallon mild steel drums. The waste was usually mixed with or encased in cement prior to or at the time of packaging so that the average package density was sufficiently greater than seawater to ensure sinking to the ocean floor after disposal. The drums served to contain the waste mixtures, to minimize dispersion during handling and transportation and to offer some radiation protection to personnel. No credit was given to the container as a barrier to radionuclide migration in ocean disposal. It was assumed that all the radioactive materials would eventually be released since the packages were not designed or required to remain intact for sustained periods of time after descent to the ocean floor. It was further assumed that ocean currents would dilute and disperse the radioactivity to such low concentrations that it would not constitute a significant hazard to man and the environment.

Several of the techniques used for packaging radioactive wastes which were deposited in the Farallon Islands disposal site are shown in Figure 1.2.

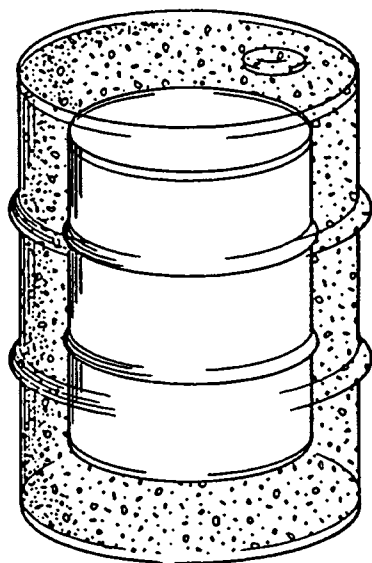
Beginning in 1951-52, all radioactive waste packages for ocean disposal at the Pacific site incorporated a lifting eye which consisted predominantly of a wire rope or a bent steel reinforcement bar with both ends embedded into an exposed concrete cap. This information was useful in identifying and dating radioactive waste packages during the EPA surveys at the 900-meter subsite in 1974-75 and at the 1700-meter subsite in 1977.



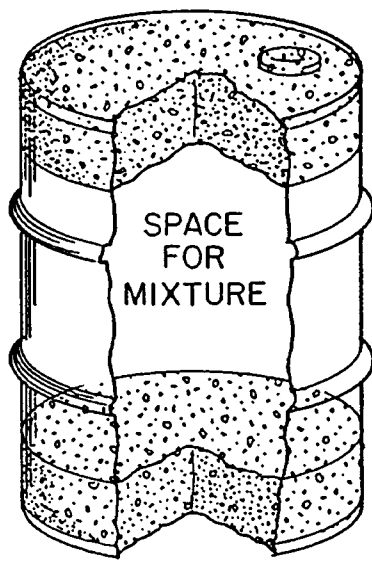
(a)  
Weighted drum for  
low level liquids



(b)  
Carboy of low level  
liquids



(c)  
30 gallon drum of  
solidified liquids



(d)  
Mixture of solid waste  
materials and concrete

Figure 1.2 Cut Away Isometric Views Showing Modifications of 55-Gallon Drums for Packaging Radioactive Wastes Which Were Disposed of In The Farallon Islands Disposal Site

## 2. SURVEY AND RECOVERY OF A WASTE PACKAGE FROM THE 900-METER SITE

The framework for the eventual recovery and analysis of a waste package from the Pacific Ocean began in 1974, when EPA successfully conducted an environmental assessment survey of the radioactive waste disposal site near the Farallon Islands [3].

The survey was conducted primarily to determine the fate of radioactive waste packages disposed of at that site between 1946-65, and to make preliminary determinations regarding the distribution of any released radioactivity.

### 2.1 FARALLON ISLANDS 900-METER DISPOSAL SITE SURVEY (1974)

The 900-meter site (Figure 1.1) was selected by EPA as the first in a planned series of ocean disposal site surveys in the Pacific and Atlantic Oceans. The site was singled out in preference to others because (1) it was the only site used exclusively for disposal of radioactive waste, (2) it was used only from 1951-53, (thereby allowing estimates of the age of the waste package and the rates of biofouling and corrosion), and (3) the precise coordinates of the site were known.

The site survey was conducted through the use of the Cable-controlled Underwater Recovery Vehicle (CURV III), operated by the U.S. Navy Undersea Center (NUC) in San Diego. The CURV III, shown in Figure 2.1, is a tethered, unmanned submersible which is remotely controlled from shipboard and has capabilities for both sediment sample collection and photographic documentation. Its equipment includes two movable television cameras, a 35mm color camera with synchronized strobe, and a sonar system capable of scanning an area of 120° and detecting waste packages at distances up to 400 meters [4].

On August 28, 1974, the first cluster of waste packages, consisting of 55-gallon mild steel drums was located. The characteristic lifting eyes positively identified them as radioactive waste packages disposed of 21-23 years earlier.

Although a pronounced number of packages appeared to have imploded due to hydrostatic pressure, none of the observed packages showed signs of having been breached solely from external corrosive forces, even though some surface corrosion was evident on the containers. The hydrostatic implosions were the consequence of air voids and/or the nonhomogeneity of the waste form within the container when exposed to deepsea high pressure conditions. The condition of some waste packages observed during this survey are evident in a series of color photographs contained in an EPA operations report [1].

This preliminary survey established the feasibility for conducting more sophisticated studies at radioactive waste disposal sites and laid the groundwork for subsequent surveys which were conducted in 1976-78 at other subsites in the Pacific Ocean and at Atlantic Ocean disposal sites.

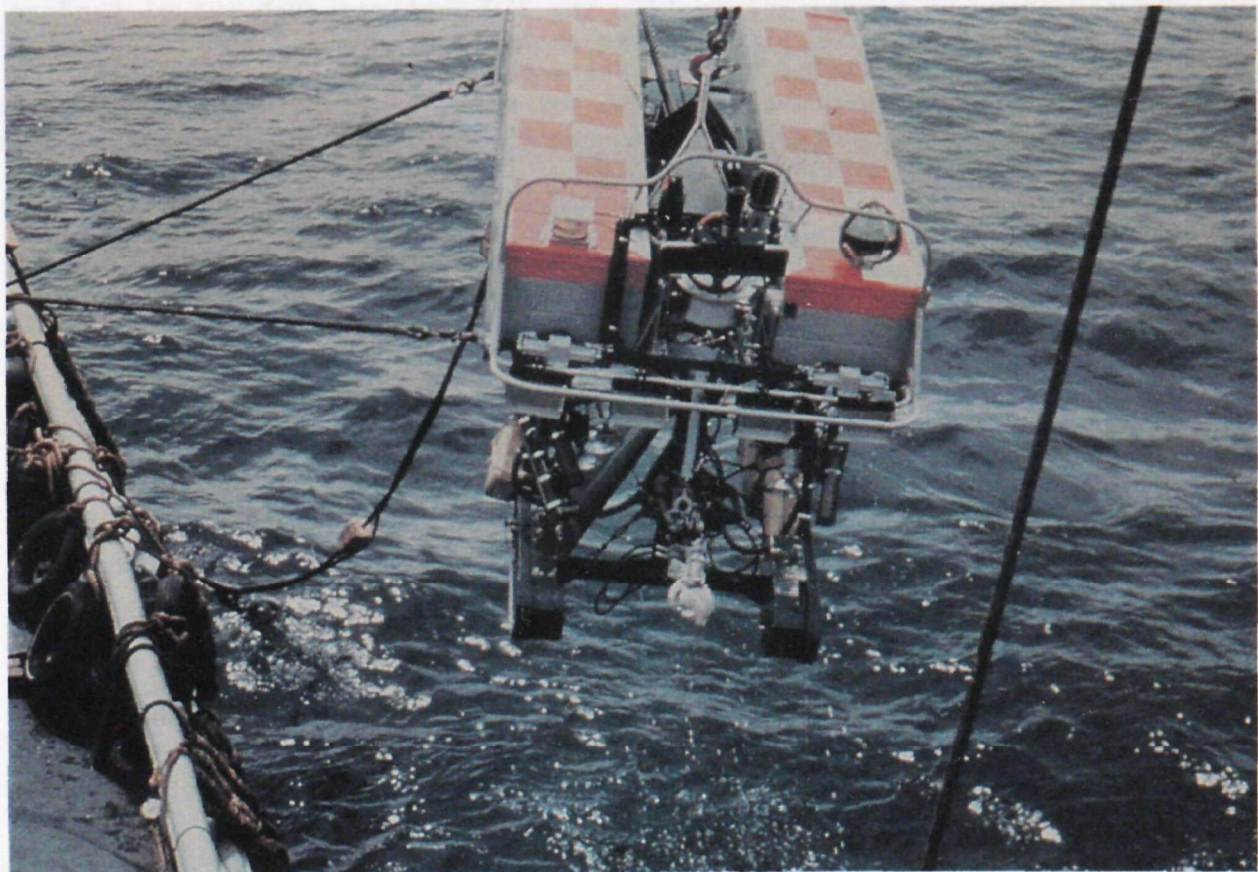


Figure 2.1 Unmanned Cable Controlled Underwater Recovery Vehicle, CURV III



## 2.2 RETRIEVAL OF A WASTE PACKAGE FROM THE FARALLON ISLANDS 900-METER SUBSITE (1977)

In October 1977, a second survey of the Farallon Islands 900-meter disposal site was undertaken by EPA for the specific purposes of: (1) retrieving a radioactive waste package and (2) supplementing information acquired during the 1974 survey regarding the geochemical, radiochemical, and biological characteristics of the site.

### 2.2.1. Retrieval Operation

The retrieval of a waste package from the 900-meter site was a coordinated effort involving the research vessel Pandora II, the manned submersible PISCES VI, and the research vessel Velero IV. The 220-foot research vessel Pandora II was the support ship for PISCES VI as shown in Figure 2.2 and is operated by the Canadian Department of Fisheries and the Environment. On October 17, 1977, it arrived from Vancouver, British Columbia, to Fisherman's Wharf in San Francisco, California, where it joined the 110-foot research vessel Velero IV of the University of Southern California for a scheduled 10-day study at the Farallon Islands disposal site. Figure 2.3 shows the highly specialized Canadian research vessel Pandora II with its large articulated A-Frame for raising and lowering the submersible. Figure 2.4 shows the research vessel Velero IV, from which correlating biological, geological, and radiochemical data were collected. The Velero IV was also designated for shipboard recovery of a radioactive waste package.

On October 21, 1977, a pre-recovery survey was conducted at the 900-meter site to select a waste package for recovery.

The criteria established for the selection and recovery of the waste package included the following:

- It should have identifiable markings regarding its source, activity level and date of disposal.
- It should be essentially intact with no signs of implosion or breaching due to impact with the ocean floor; this would minimize the possibility of shipboard and personnel contamination during recovery.
- The exposure rates (as measured from the manned submersible prior to recovery) should not be of a level which might affect the health and safety of personnel during recovery, storage, and transportation.

The precise positioning of sighted radioactive waste packages and the accuracy with which depths were recorded during the 1974 survey of the 900-meter site identified the areas having appreciable numbers of waste packages. This earlier information not only served to pinpoint locations but also provided the opportunity to select a waste package which could best represent the effects of the ocean environment during the time it sat on the ocean floor.



Figure 2.2 Manned Submersible PISCES VI





Figure 2.3 Canadian Research Vessel PANDORA II



Figure 2.4 University of Southern California Research Vessel VELERO IV

During the course of this survey, photographs were taken by PISCES VI for documentation and for verification of the condition of the drums observed during the 1974 survey of the 900-meter site.

An example of the implosion pattern characteristic of many of the waste packages sighted is shown in Figure 2.5. Hydrostatic crushing at the center of a drum is typical of radioactive waste packages prepared as shown in Figure 1.2, whereby the waste was essentially sandwiched between two plugs of concrete within the container. Invariably the waste consisted of laboratory trash which was insufficiently compacted to remove air voids or lacked the physical strength to resist hydrostatic implosion. Although the center portion of the drum in Figure 2.5 showed severe indentations, it did not appear to be breached. Several thornyhead fish, either Sebastolobus alascanus or Sebastolobus altivelis are seen taking shelter near the side of the drum. The exposed concrete cap establishes a solid anchor site for a number of marine invertebrates such as the white vasiform hexactinellid sponges attached to the exposed concrete end of the package.

Figure 2.6 shows a waste package with a moderate amount of hydrostatic crushing. A lifting eye, typical of waste packages disposed of at the site between 1951-1953, is evident on the concrete end of the package. Also evident are several sponges attached to the concrete.

By contrast, Figure 2.7 shows a barrel with no evidence of hydrostatic crushing. A coating of fine, minimally disturbed sediment is prominent on the exterior of the drum. Sediment taken by boxcore in the vicinity of this drum is sandy silt having a mean grain size of approximately 5.6 $\phi$ . At the surface the sediment consists of 28.8 percent sand, 44.8 percent silt and 26.8 percent clay [5]. The photo also indicates the small amount of drum penetration into the sediment with little or no sediment scouring in the vicinity of the drum.

The waste package shown in Figures 2.8 and 2.9 was selected for recovery since it closely complied with the aforementioned selection criteria and it appeared to be in good enough condition to survive the trip to the surface and yet provide meaningful information on past packaging technique. Figure 2.8 shows the mechanical arm of the PISCES VI carefully rolling the drum to ensure that it was not breached on its underside. The concrete cap and lifting eye of the waste package, as seen in Figure 2.9, was inspected to ensure that they would remain intact during the attachment of the lift line to the lifting eye and recovery of the waste package from the ocean floor. In both Figures 2.7 and 2.8, some of the benthic and demersal fish population can be seen close to the waste packages.



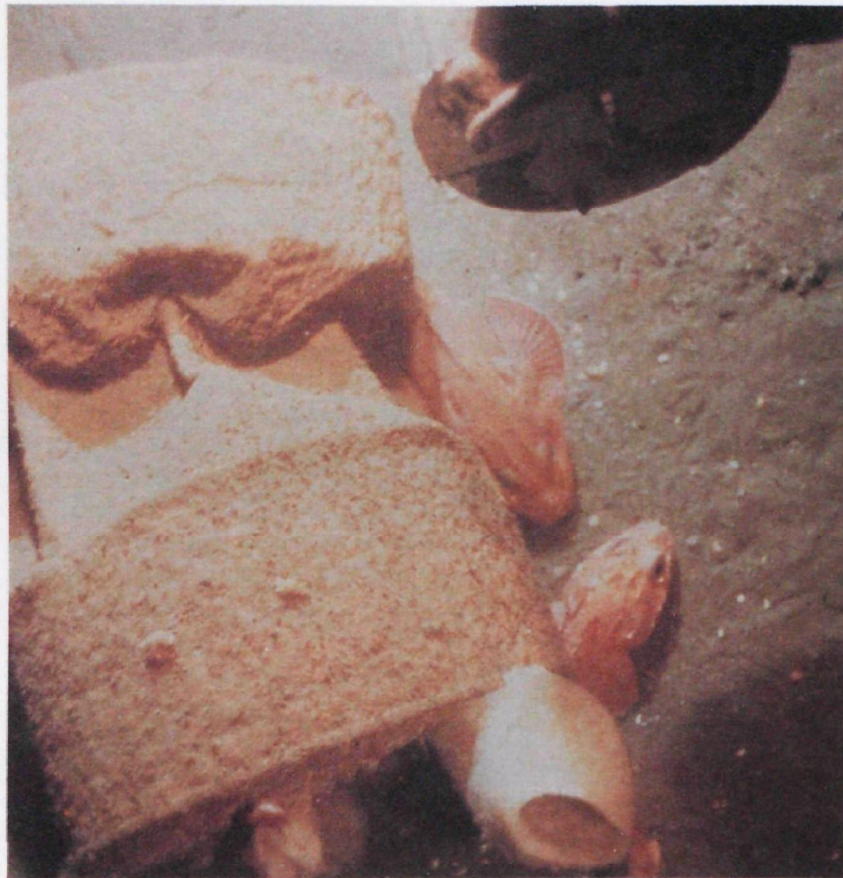


Figure 2.5 Waste Package Showing Severe Hydrostatic Implosion



Figure 2.6 Waste Package Showing Mild Hydrostatic Implosion





Figure 2.7 Waste Package Showing No Signs of Hydrostatic Implosion





Figure 2.8 Underwater Inspection of Recovered Waste Package

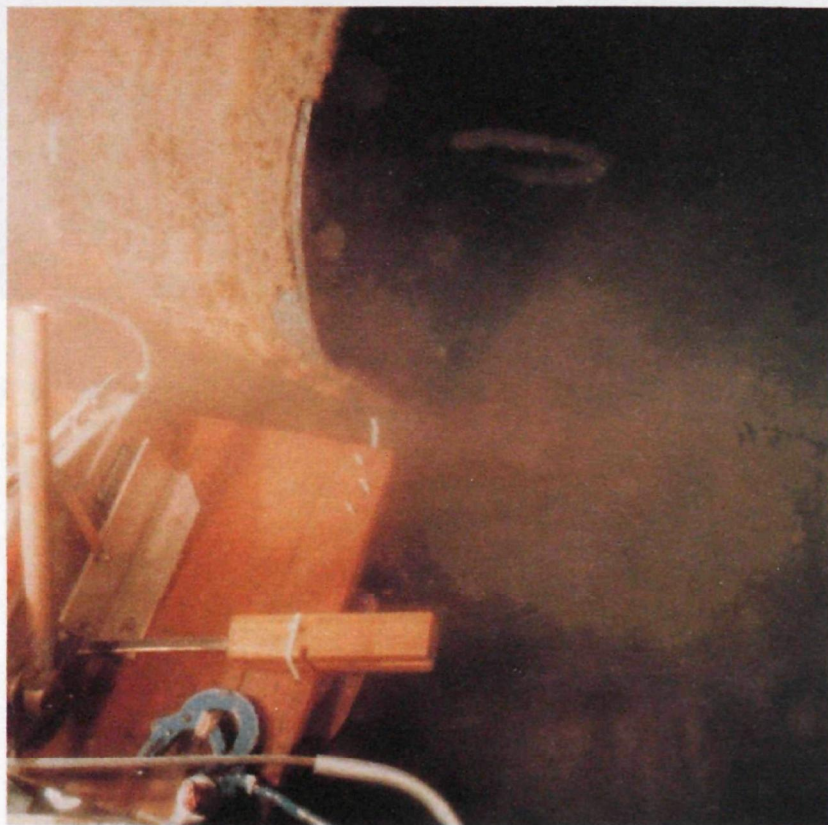


Figure 2.9 View of the Wire Rope Lifting Eye Imbedded into the Concrete Waste Form

On October 22, 1977, at 0927 hours, the PISCES VI, Figure 2.10, was launched to recover the waste package which had been selected by visual observation from the submersible the previous day. The PISCES VI arrived at the site of the selected package at 1150 hours. The depth of the water was 915 meters (approximately 2,750 feet). The PISCES VI proceeded to capture the package by placing a metal harness over the top of the package. The mechanical arm of the submersible secured the harness around the package using a grip hoist which cinched the wire rope of the harness around the package. Although the same procedure was used for harnessing the package for recovery from the Atlantic Ocean 2800-meter site in 1976 [6], the package was raised by connecting it directly to a winch line from the recovery vessel. In the current case, the package was lifted using two nylon ropes attached to the submersible. At 1420 hours, the PISCES VI was off the bottom and pumping ballast to ascend. The package was reported free from the bottom at 1445 hours and the PISCES VI surfaced at 1536 hours. At 1600 hours, Velero IV closed for the package recovery and by 1610 hours all lines were attached from the package to the recovery ship. At 1613 hours, the package was released from the PISCES VI and recovery operations aboard the Velero IV began. By 1700 hours, the waste package broke the surface of the water. Before bringing it aboard, it was allowed to drain while at the same time it was subjected to a radiation survey by the health physicist aboard the Velero IV.

#### 2.2.2. Radiation Surveillance

The necessary monitoring equipment for alpha-beta-gamma counting was assembled and calibrated before taking it aboard the research vessel Pandora II in preparation for the survey and recovery operations. Radioactive standard sources also were taken along for periodic checking and recalibration of the monitoring equipment.

Prior to the survey and recovery activities, a radiation safety lecture was given to the crews of the PISCES VI and the research vessel Pandora II and the research vessel Velero IV. This lecture included radiation exposure limits, radiation contamination, biological effects of radiation, procedures for the use of film badges, self-reading dosimeters and survey meter operations. The operators of the PISCES VI carried a radiation survey instrument aboard during each dive. After each dive, the health physicist performed a contamination survey of the PISCES VI and the Pandora II to detect any radioactive contamination in samples collected and sampling equipment used during the disposal site surveys.

Prior to retrieval operations aboard the research vessel Velero IV, preparations were made to prevent radiation exposure or the spread of radioactive contamination in the event of leakage or an accident during the recovery operations.



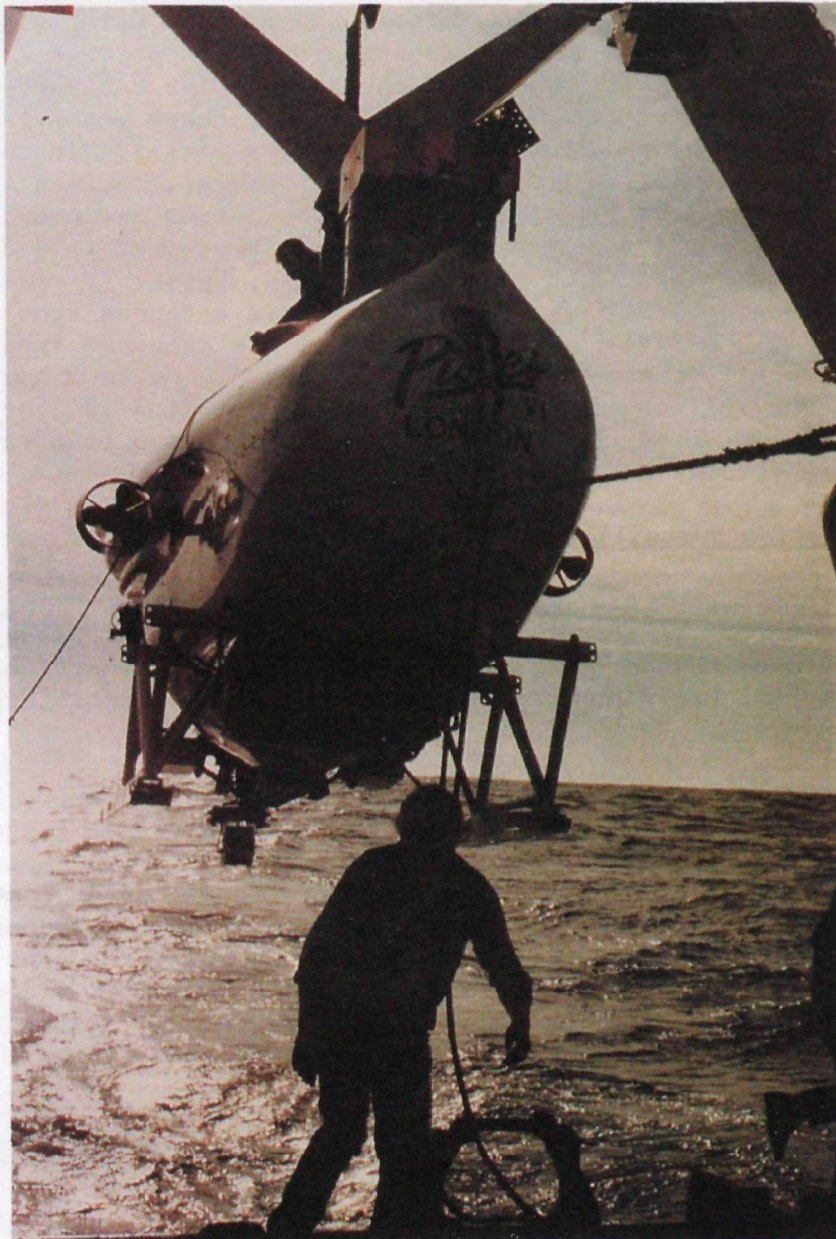


Figure 2.10 Submersible PISCES VI Being Launched For Waste Package Recovery

A collision mat was secured to the ship's transom with a double protective cover consisting of a heavy duty nylon reinforced polyethylene tarpaulin on the bottom and a canvas tarpaulin on the top, as shown in Figure 2.11. The tarpaulins served to reinforce the collision mat and to confine "run-off" in the event that water was discharged from the waste package during pressure equalization or from void pockets within the package. It should be noted that the pressure exerted on the surface of the waste package at a depth of 900 meters is approximately 1500 psi. The tarpaulins were extended from the transom inboard to cover an area beyond that required to accommodate the waste package. A 2-inch thick open cell polyurethane slab was then secured in position to receive the waste package as shown in Figure 2.12. The purpose of the open cell polyurethane slab was to: (1) act as a cushion for minimizing damage while lowering the waste package from the winch to the deck in rolling seas, (2) absorb any aqueous run-off from the waste package, and (3) facilitate containment of any radioactivity by rolling and properly wrapping the flexible polyurethane slab.

Before the retrieval operations began, the health physicist and the monitoring equipment were transferred from the Pandora II to the Velero IV. The shipboard area designated to receive the waste package was restricted to the health physicist and to personnel specifically assigned to assist in the retrieval operation. This step was taken to minimize potential contamination and personnel radiation exposure during shipboard operations. During the recovery operation, a preliminary radiation survey of the package was performed before taking it aboard and while it was suspended over the stern of the Velero IV. This was followed by a complete radiation and contamination survey after it was taken aboard.

The recovered package showed no external radiation or contamination. Smear samples of the research vessel Pandora II, Velero IV, and the submersible PISCES VI showed no contamination during or at the conclusion of operations. The film badges and self-reading dosimeters worn by personnel involved in the survey and recovery operations showed no radiation exposures above background.





Figure 2.11 Waste Package Being Hoisted Aboard the Research Vessel VELERO IV



Figure 2.12 The Waste Package Being Prepared for Visual Inspection

### 2.2.3. Shipboard Inspection

Immediately after being hoisted on board the waste package was secured to the deck of the ship where it was photographed and sampled for corrosion products and biological growth. Sediment adhering to the bottom side of the package was also sampled.

The mud, which clung strongly to the container during retrieval, appeared greenish-black in color and had a faint odor of hydrogen sulfide, indicating an anoxic environment. The pH of the sediment, measured with indicator paper, was between 8-10. The mud line can be seen on the upper side of the concrete face in Figure 2.11.

The sea-exposed surface of the container contained corrosion products and scale ranging in color from black to reddish orange, as seen in Figure 2.13. The whitish areas around the rim of the container in Figure 2.13, resemble polychaete (sea worm) tubes. Sea worms appear to be prominent as observed on the concrete surface in Figure 2.14. In addition to the worms, several small or broken sponges can be seen attached to the concrete surface.

In general, the condition of the container appeared to be good considering the duration of exposure in the deep ocean (estimated 21-23 years). The area of heavy corrosion appeared to be on the outer rim of the sediment side of the container. A more detailed description of the types and effects of corrosion on the metal container will be given later in this report.





Figure 2.13 A View of the Corrosion on the Sea Side of the Container



Figure 2.14 Sea Worms Attached to the Concrete Surface of the Waste Form

#### 2.2.4. Storage and Transportation

The on-board inspection of the waste package was limited to approximately one hour to minimize any chemical changes which might occur in an oxygenated environment. Following inspection, the metal capture harness was removed and the waste package was sealed into a cylindrical steel storage container, which was especially designed to accommodate a standard 55-gallon drum. The container conformed with all Department of Transportation (DOT) criteria for Type A packages except for pressure requirements. Modifications were made to provide a gasket seal between the cover flange and the flange of the container which complied with the DOT requirements for maintaining the prescribed over-pressure.

The cover of the storage container was further modified to provide the necessary hardware for introducing an inert gas (argon) to replace the air in the container. The use of inert gas was to minimize further corrosion of the metal container during storage and transportation. Air was removed from the storage container by continuously feeding argon gas into the container until the oxygen concentration in the exit gas was reduced to 0.5 percent. The gas inlet and outlet valves were then sealed to maintain a pressure of argon gas slightly above atmosphere.

At the point of debarkation, (San Francisco, California), the storage container accommodating the waste package, was placed into an overpack for transportation to Brookhaven National Laboratory. The overpack used is a DOT approved metal container suitable for the transportation of B type (transuranic) waste. Because the radioactive content of the waste package was not known following recovery, the above special transportation options were used to assure compliance with regulations regarding the handling and transportation of such wastes.



### 3. ANALYSIS OF THE CONCRETE WASTE FORM

The recovered waste package consisted of a conventional 55-gallon mild steel drum filled to within 1.5-2.0 inches from the top with a concrete mix. Protruding through the exposed concrete end was a wire rope lifting eye which was firmly embedded into the concrete. Although the overall appearance of the metal container was good, the corrosion on the sea side appeared to be highly localized. The nonuniform corrosion was surprising in that one would expect a more even distribution. However, since most of the drums were used or reconditioned prior to packaging and disposal, a large degree of uncertainty exists regarding the initial conditions of any individual container and the effects of the ocean environment on the corrosivity of the waste containers.

The blackish mud, indicative of anaerobic bottom conditions, remained strongly bonded to the container when it was removed from the sealed storage container, as shown in Figure 3.1. A faint odor of hydrogen sulfide could be detected, typical of anaerobic bottom sediments where sulfate-reducing bacteria are present. This condition is initiated through the formation of ferrous sulphide ( $\text{FeS}$ ) scale on the steel, which is cathodic to the bare metal surface [7,8].

When the waste package was exposed to atmospheric conditions, the blackish coloration immediately began to change to greenish-brown, as shown in Figure 3.2. This can be attributed to oxidation processes, with some metals such as iron, during the transition from anaerobic to aerobic conditions.

A pool of liquid was observed at the bottom of the shipping container upon removal of the waste package. This liquid, consisting of 13 liters, was immediately collected for radiochemical analysis and pH determination. It was presumed that the liquid had drained from the waste form since the shipping container was hermetically sealed during storage and transportation. Such a volume of liquid would require an appreciable void space to accommodate it within the waste form. From this it was hypothesized that a packaging technique along the lines of that demonstrated in Figure 1.2 (b) had been used to package the waste.

#### 3.1 RADIOGRAPHY

During the analysis of the waste package which was recovered from the Atlantic 2800-meter disposal site in 1976 [6] it became apparent that radiographs can provide the necessary information to determine the presence and location of objects which were incorporated into the cement waste form for disposal.

Radiographs for this study were produced using a 45-curie cobalt-60 source supplied by the Consolidated Testing Laboratories, Inc., New Hyde Park, New York. Since the waste form was suspect, a total of four sides of radiographs were taken with the source located on the 0°, 90°, 180°, and 270° longitudinal axis of the drum. Fiducial markers were placed on the drum to allow the subsequent positioning of one radiograph relative to another.

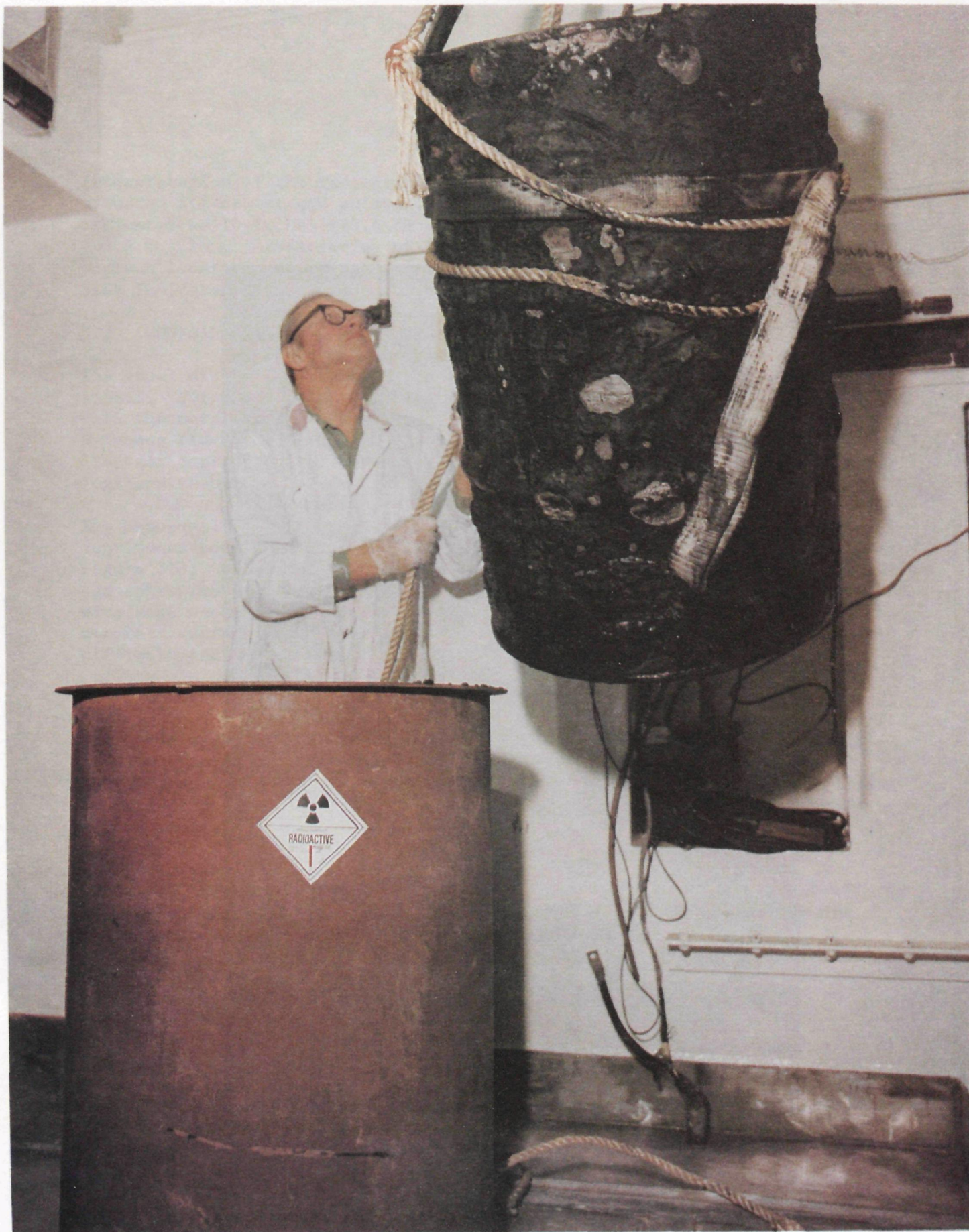


Figure 3.1 Removal of the Waste Package From the Shipping Container





Figure 3.2 View of the Sediment Side of the Waste Container



Interpretation of the radiographs indicated a rectangular-shaped cavity situated off-center and adjacent to the 270° line. The size of the void was estimated as 10 inches (25.4 cm) wide x 10 inches (25.4 cm) high x 12 inches (30.5 cm) long. Positioning of this cavity permitted cores to be taken at various locations and depths without impacting the void area. The radiographs also indicated the precise location of the deeply embedded wire rope ends.

### 3.2 CONTAINER REMOVAL

The steel drum was carefully removed from the waste form using a pneumatic chisel. For maintaining continuity, the same orientation system was used for both the metal container and the concrete waste form. Longitudinal sections, 4 inches (10.2 cm) wide, were cut from the drum above and below the sediment line for corrosion analysis. More detailed descriptions of the metal samplings and results are given in Section 4 of this report.

The homogeneity of the concrete, along its entire length, indicated that a continuous pouring was made in preparing the waste form. This is shown in Figure 3.3. Since the radiographs indicated that the upper side of the cavity was approximately 8.5 inches (21.6 cm) from the exposed concrete surface, the wire rope was cut and an attempt was made to reach the cavity by probing the concrete surface. The hardness of the concrete, however, made this task difficult and it was decided to use coring equipment.

### 3.3 CONCRETE CORING

The cores were obtained using a concrete hole saw with a dual speed motor (500/100 rpm) on a swivel base [6]. Two-inch cores were obtained using impregnated diamond core bits. Water was sparingly used during the drilling operations as a lubricant and to minimize dispersion of fines. With this method, cores were obtained having 2 inch (5.1 cm) diameters and 4 inch (10.2 cm) lengths. Cores were taken along the 0°, 90°, 180° and 270° longitudinal axes at distances of 5.25 inches (12.7 cm), 16 inches (40.6 cm) and 26.5 inches (67.3 cm) from the top of the concrete waste form. The concrete cores were taken to determine the compression strength of the concrete and for radiochemical analysis.

Prior to obtaining the cores, exploratory drillings were conducted to substantiate the location of the cavity as indicated by the radiographs and to determine the contents of the cavity.

The cavity was located at a depth of 8.5 inches from the top of the waste form, as indicated by the radiograph. Using a steel-hooked rod, pieces of cardboard were extracted from the cavity. The same material was extracted from drill holes made along the periphery of the cavity. During this operation, all extracted materials were continuously surveyed for radioactivity.





Figure 3.3 Concrete Waste Form After Removal of Container



Based on the estimated location of the cavity, it was decided to attempt cutting the waste form along the upper chime line as demarcated by the 55-gallon metal drum which according to the radiograph, coincided with the estimated center of the cavity. The waste form was finally parted using a pneumatic chisel.

#### 3.4 WASTE CONTENT

Figure 3.4 shows the parted waste form and the cavity, which housed a thick, empty cardboard container. Figures 3.5 and 3.6 show a closeup of the parted waste form. Note the integrity of the cardboard and the legibility of the print in Figure 3.6.

The cardboard box was carefully removed from the cavity to determine if it contained any information which might shed some light on its original contents. The following markings were identified on the side and bottom of the box.

##### SIDE OF BOX

TOP  
HANDLE WITH CARE  
GLASS  
NET 35 LBS  
GR 54 LBS  
NO. 4052

##### BOTTOM OF BOX

3 GALS  
1  
1006  
1048  
0

The certification seal, also located on the bottom of the box read:

GAIR BOGATA CORP.  
CERTIFICATE OF BOX MAKER  
THIS BOX CONFORMS TO ALL CONSTRUCTION REQUIREMENTS  
OF CONSOLIDATED FREIGHT CLASSIFICATION  
BURSTING TEST 200 LBS PER SQ. INCH  
SIZE LIMIT \_\_\_\_\_ 5 INCHES  
GROSS WT. 65 LBS  
BOGATA N \_\_\_\_\_



Figure 3.4 View of the Position of the Cardboard Box Embedded in Cement





Figure 3.5 Closeup of Parted Waste Form



Figure 3.6 Legibility of Printed Matter on Cardboard Box

### 3.5 RADIOACTIVITY

No radioactivity was detected in samples taken during each phase of this operation. This included shipboard smears of the waste package and analysis of the discharged liquid, the cardboard box, and the concrete cores. Yet, the evidence is there to indicate that historically the recovered waste package was disposed of at sea as radioactive waste. In view of this, the following can be postulated:

- (a) The cardboard box was discarded as "suspect" waste and was not radioactive at the time of packaging. The practice of combining "suspect" waste with radioactive contaminated waste was prevalent in most laboratories since it eliminated the task of performing radiological assays and segregation of the waste.
- (b) The cardboard box was contaminated with short half-lived radionuclides. It seems unlikely that a concrete casting was made specifically to house an empty cardboard box unless the box was heavily contaminated with radioactivity. In the absence of any detectable radioactivity it can be presumed that the contaminants consisted of one or more short-lived radionuclides.
- (c) All of the radioactivity leached out of the waste form. Judging by the integrity of the cardboard box, the concrete waste form and the container, it is difficult to visualize that all of the activity leached out of the waste form. This is unlikely based on several facts. The cardboard box, the concrete waste form and the containers had maintained their integrity during 22 years of disposal. This would impede leaching. Other waste forms recovered from ocean disposal sites had significant quantities of radionuclides present after periods of up to 16 years. A diffusion coefficient of  $10^{-7}$  cm<sup>2</sup>/sec is a typical, high release rate observed for concrete waste forms in seawater. With this rate, assuming diffusion as the release mechanism, a homogeneous waste form having the dimensions of the recovered package would still retain 34 percent of its activity after 22 years. If it can be assumed that the activity were originally contained in the vicinity of the cardboard box, then significantly more than 34 percent of the activity would be retained.

### 3.6 WASTE FORM INTEGRITY

The durability of the waste form in the ocean environment was determined by measuring the compressive strength of concrete cores taken along its longitudinal axes, as described in 3.3 of this report. The tests were conducted using ASTM Standard C 39-72, "Method of Test for Compressive Strength of Cylindrical Concrete Specimens." Table 3.1 lists the average compressive strengths of the tested cores.

Although the original concrete formulation is not known, dissolved core samples were analyzed to determine the mix proportions used to produce the concrete. The results indicated that the mix consisted of 49.2 wt. percent aggregate (crushed rocks), 30.5 wt. percent sand and 13.3 wt. percent portland cement. From this, it was estimated that 6.8 wt. percent was water, having a water to cement ratio of 0.5.

It is difficult to predict the effects of the ocean environment on compressive strength since the initial values are not known. However, the waste form did not exhibit attack due to the chemical action of the dissolved salts in seawater, to mechanical attrition, to the corrosion of the metal container, or to bacterial actions. This is surprising since sulfates in seawater attack cements very markedly. The conversion of calcium hydroxide ( $\text{Ca}(\text{OH})_2$ ) to gypsum ( $\text{CaSO}_4 \cdot 2\text{H}_2\text{O}$ ) through sodium or calcium sulfate attack more than doubles the solid volume, resulting in the expansion and deterioration of the cement. Magnesium sulfate, however, forms a hard dense skin on concrete surfaces and tends to hinder penetration of sulfate solutions by depositing magnesium hydroxide in the cement pores.

Although these compounds ( $\text{Ca}(\text{OH})_2$ ,  $\text{CaSO}_4 \cdot 2\text{H}_2\text{O}$ , and  $\text{Mg}(\text{OH})_2$ ) were detected in varying concentrations both on the surface of the concrete and within the concrete form, it is difficult to predict the reaction mechanisms or the rates of formation under the conditions to which the waste form was exposed to over the 21-25 year period.



TABLE 3.1

COMPRESSIVE STRENGTH OF CONCRETE CORES

<u>Longitudinal Axis</u>	<u>Distance from top of Waste Form, in.</u>	<u>Core Size, in. (d x l )</u>	<u>Compression Strength psi (average)</u>
0°	(5.25, 16.0, 26.5)	1.73 x 3.85	2,780
90°	(5.25, 16.0, 26.5)	1.73 x 3.96	2,850
180°	(16.0, 26.5)	1.73 x 3.92	2,790
270°	(26.5)	1.73 x 3.87	2,760

#### 4. CORROSION ANALYSIS OF THE METAL CONTAINER

From the previous corrosion analysis of the waste package retrieved from the 2800-meter disposal site in the Atlantic Ocean [6], a well-defined procedure has been developed. This procedure includes, when possible, those tasks outlined in the National Association of Corrosion Engineers (NACE) Standard RP-01-73 describing recommended practices for collection and identification of corrosion products [9].

The package was kept in an inert argon atmosphere from the recovery to commencement of analysis. However, once analysis commenced, the trepanned samples and surface scrapings were kept in a desiccator prior to physical analysis.

The task sequence for corrosion analysis is as follows:

Task I: Visual Inspection. Visual inspection of the overall container, sampling of scale, pH, and sediment provides an early qualitative record of the container and samples for further analysis. Also, coordinates to which samples are indexed are defined.

Task II: Dimensional Analysis. The inspection resulting from Task I allows selection of areas on the sea side and sediment side from which strips of material are cut. Sections from these strips are mounted in epoxy for cross-section dimensional analysis. In addition, samples are trepanned from sites of specific attack or protection. Estimates of corrosion rates as a function of position result from this analysis.

Task III: Micro-Analysis. The analyses made in Task I and II pinpoint specific sites of either high protection or high corrosion rates for further microscopic scrutiny. Optical and scanning electron microscopic techniques provide metallographic evaluation of cross sections and surface morphology at points of either high local failure or enhanced protection.

Task IV: Chemical Analysis. In parallel with Task III, X-ray diffraction (XRD), X-ray fluorescence spectroscopy (XFS), and bulk chemical analysis provide information on the local and bulk chemistries involved in the corrosion protection mechanisms.

The corrosion analysis takes as its objective an assessment of the effect of the disposal site environment upon the carbon steel sheathing material. In addition, the results of this analysis will determine specific instances of protection or failure thereby providing input for future practices.

##### 4.1 VISUAL INSPECTION AND SAMPLING

Figure 4.1 is a schematic of the coordinate system ( $x$ ,  $r$ ,  $\theta$ ) used to specify locations on the container. The coordinate  $x$  specifies the distance parallel to the cylindrical axis from the end containing the exposed waste form. The  $r$  coordinate is the radial distance from the cylindrical axis; the surface of

the carbon steel sheath, therefore, is at  $r \approx 11.25$  inches (28.6 cm). Looking down the cylindrical axis from the open end, the angle,  $\theta$ , is in degrees clockwise from an initially marked  $0^\circ$  position. The cylindrical container, Figures 4.2-4.5, has an average diameter of 22.5 inches (57.2 cm) and an average length of 34.9 inches (68.6 cm).

As seen from Figure 4.2, the portion of the container buried in black mud comprises those coordinates between  $\approx 0^\circ$  and  $\approx 135^\circ$  and the sea side comprises regions between  $135^\circ$  and  $360^\circ$ . The sea-exposed surface contains black to orange scale and corrosion products. In addition, many nodular conglomerations of orange to black corrosion products cover the sea side of the container. Figure 4.6 shows some of these regions. Where a nodule was removed an adherent black underscale was observed, characteristic of much of the other regions of the sea side (for example, Figure 4.5). Measurements using pH paper in areas where a nodule was removed indicated values between 8 and 10, corresponding to mild alkalinity. The mud also showed an alkaline pH between 8 to 10.

Black mud caked the entire portion of the mud-buried side of the container, Figure 4.2. Large spots of silvery material lie on the surface of the mud layer. Scrapings listed in Table 4.1 were taken using a porcelain spatula and stored in a desiccator.

The sheath was cut and 4 inch strips were extracted from the mud side at  $45.8^\circ$  and the sea side at  $255.8^\circ$  (Figure 4.7). Samples from these strips allowed dimensional analysis. Before cutting the container for samples, perforation of the carbon steel sheath at the rim was noted (Figure 4.8) at  $x=0$  and  $\theta=0$ .

An inside view of the container exhibited further perforation initiated along the chimes and radial corrugations (Figure 4.9), where cold work probably occurred during the forming of the drum. Figure 4.10 provides a closer view of the specific chime attack and the red to orange scale formation on the inside of the vessel. Perforation occurred on both the sea side and the sediment side and consumed 1 percent of the total container surface area.

## 4.2 DIMENSIONAL ANALYSIS

The strips cut from the respective sea and sediment sides of the carbon steel sheath provided specimens for dimensional analysis and metallographic examination. Specimens, 1 inch x 0.5 inch (2.54 cm x 1.27 cm) were extracted at 3-inch (7.6 cm) intervals along each strip. The samples were mounted in epoxy and ground past the saw cut damage with 320 paper. Photographs of these cross-sections (50 X magnification) provide a view of 0.1 inch (0.25 cm) lengths of the cross section at each 3-inch (7.6 cm) interval. The thickness from the photographed cross sections was measured at each 0.01 inch (0.025 cm) interval and averaged for a dimension determination for each 3-inch interval of  $x$ . The standard deviation of the determination depends upon the localized nature of the corrosion.

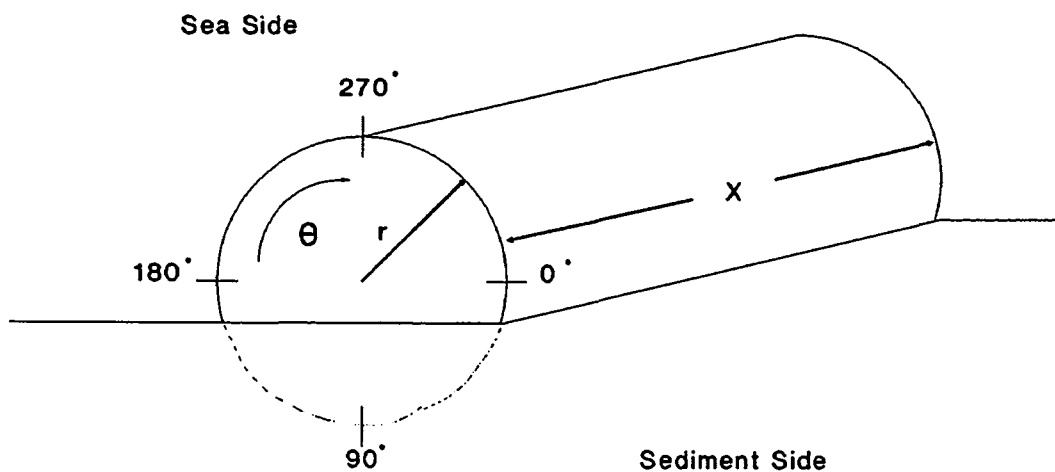


Figure 4.1 Schematic of Coordinate System Used to Identify Locations on the Container





Figure 4.2 View of Waste Package Showing the Sediment Side ( $0^{\circ}$  -  $90^{\circ}$ )





Figure 4.3 View of Waste Package Showing Sediment Sea Side Interface  
(90° - 180°)



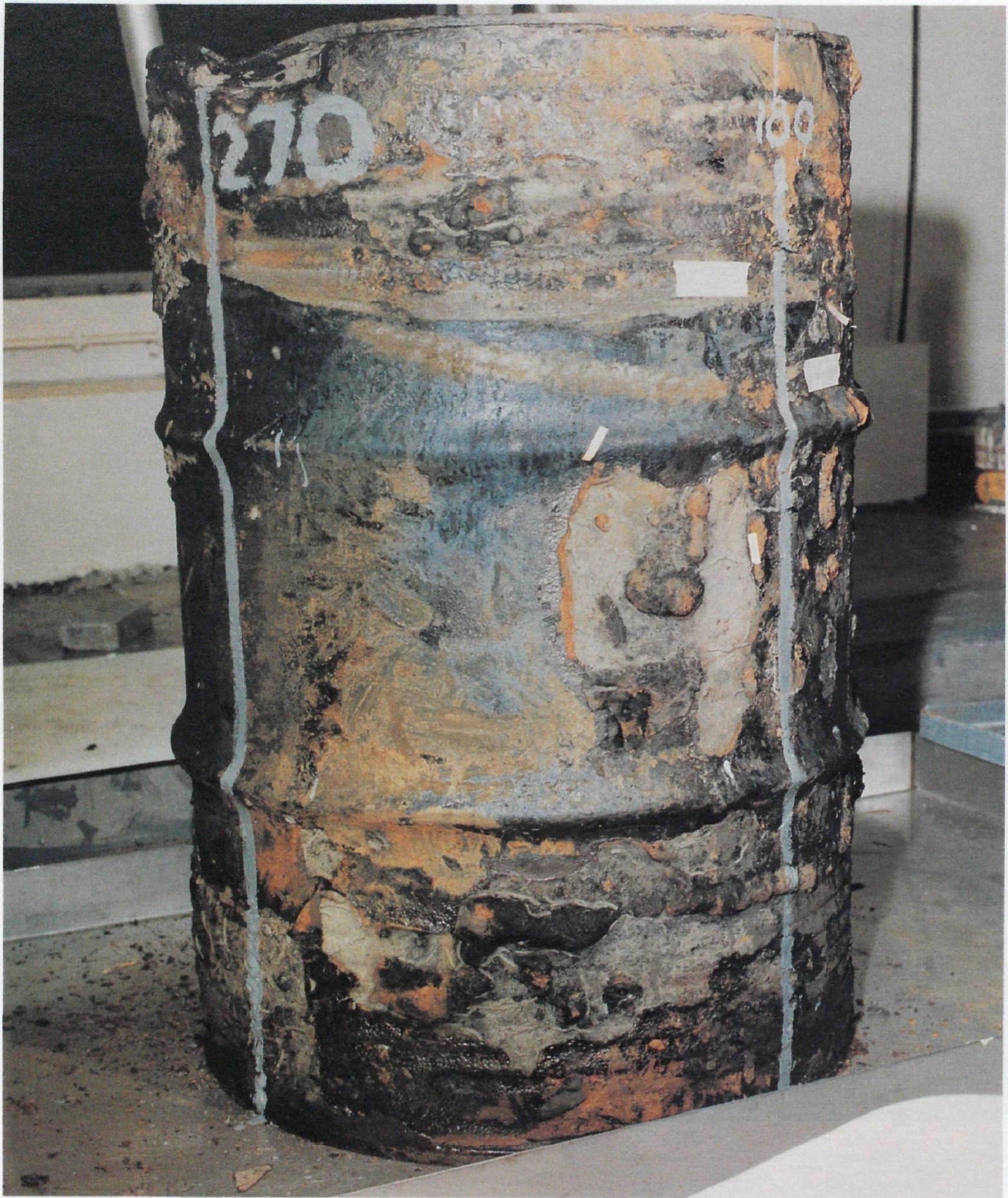


Figure 4.4 View of Waste Package Showing the Sea Side (180° - 270°)





Figure 4.5 View of Waste Package Showing the Sea Side (270° - 360°)





Figure 4.6 Nodule of Corrosion Product on Sea Side



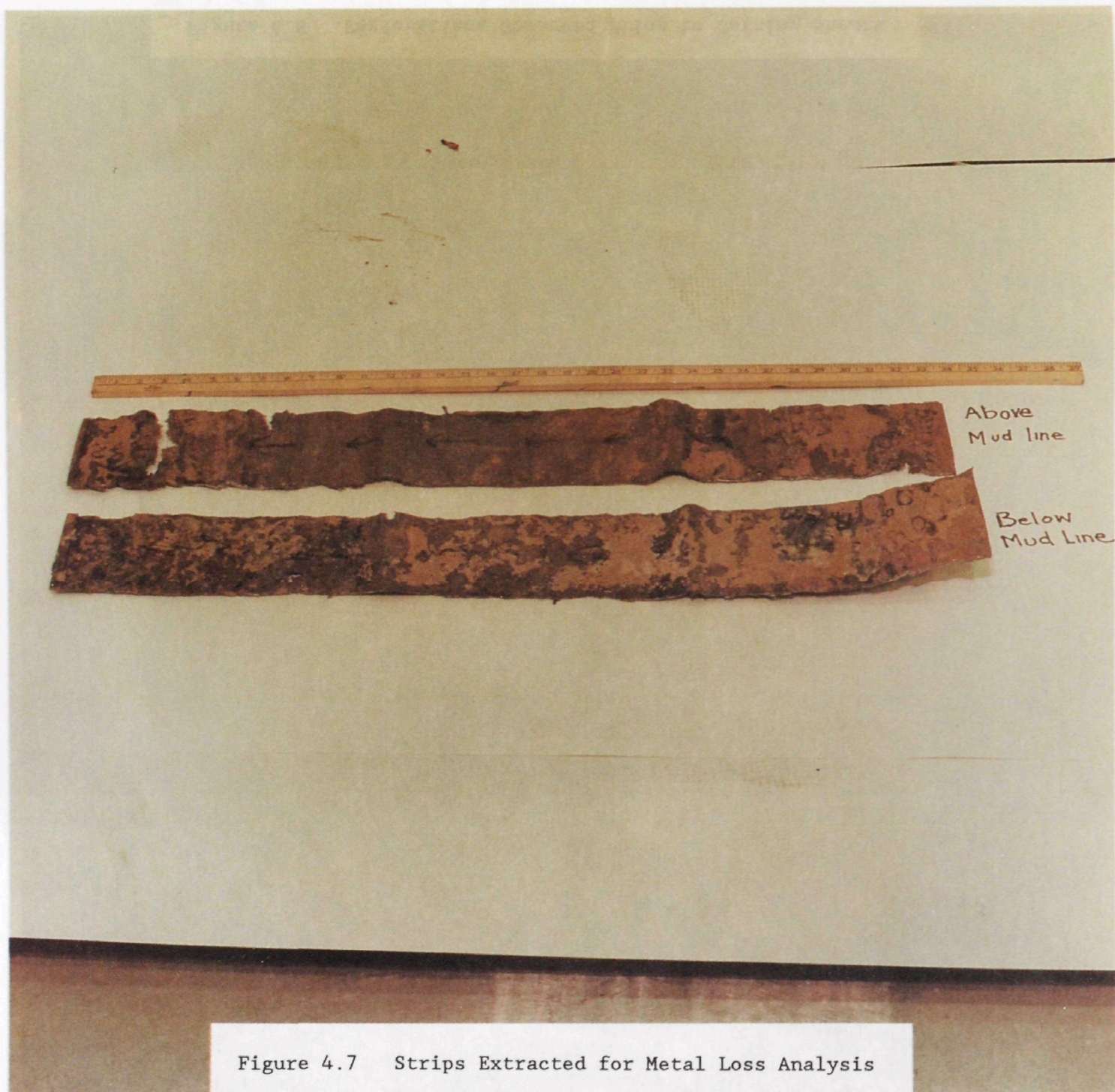


Figure 4.7 Strips Extracted for Metal Loss Analysis





Figure 4.8 Perforations Observed Prior to Cutting Sheath



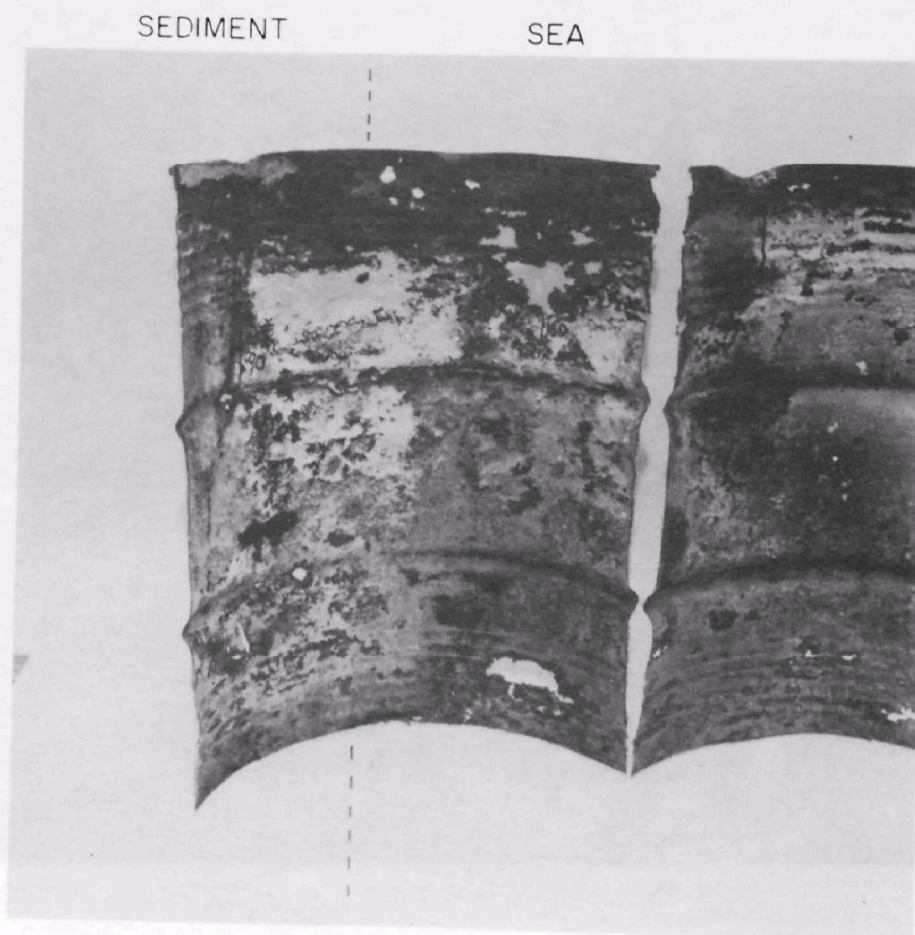


Figure 4.9 View of the Sheath from the Concrete Side





Figure 4.10 Closeup of a Chime Perforation

TABLE 4.1

SCRAPINGS

Scraping #	Position		Description
	X (cm.)	θ (degrees)	
II-1	0 to .88	0 - 270	"Silver" scale
II-2	0	0	Metal from rim
II-3	0	0 - 360	Chips
II-4	23	163	"Alkaline" nodule
II-5	32	180	Rib nodule
II-6	86	0-270	Scale and nodule
II-7	41	25	Mud
II-8	16	180	Metal near perforation
II-9	16	180	Crystalline material from perforation



Figure 4.11 shows the results plotted as metal thickness vs.  $x$ , the dimension down the container axis. As can be seen, the sediment apparently inhibits the general corrosion of the container material. The sediment side shows virtually no metal loss while the sea side shows approximately 0.045 cm average metal loss. A precise calculation of the metal loss is made difficult by insufficient knowledge of the initial thickness of the container. A fold in the rim which was presumably not attacked had a metal thickness of 0.12 cm, which was slightly less than the average thickness of the sediment side of the container. This part of the rim, however, may have been reduced somewhat by the forming process. Assuming the sediment side to have not had a significant metal loss, its average dimension may serve as the initial dimension. This average "initial dimension" is  $0.130 \pm .005$  cm. The average dimension loss for the sea side is, therefore,  $0.045 \pm 0.01$  cm.

Table 4.2 lists calculated corrosion rates based on the assumptions of (1) constant rate with (2) no induction time [10,11,12]. For this container, a rate of 0.00075 in/yr (0.019 mm/yr) for the sea side falls under those rates observed for a previously analyzed container retrieved from the 2800-meter Atlantic site. Indeed, the uniform corrosion rate of 0.00075 in/yr relates closely to the zero oxygen limit estimated from the empirical relationship of Reinhart [12]. An oxygen minimum of 0.5 cc/l exists at 900 meters off the Pacific coast near where the package was recovered. This concentration is an order of magnitude less than typical dissolved oxygen concentrations found near the Atlantic 2800 meter disposal site where a waste package was recovered in 1976. The corrosion rate may result from dissolved oxygen levels at this disposal site, but the nearly negligible corrosion rate experienced by the sediment side of the container suggests that perhaps the alkaline sediment also plays a role in suppressing general corrosion. While these measurements provide information on the general mode of corrosive attack and indicate some specific forms of attack, microscopic evaluation provides more information on mechanisms of protection or local failure.

#### 4.3 PROTECTED REGION ON THE SEDIMENT SIDE

Figure 4.12 shows micrographs of a well-protected surface at coordinates along the  $45^\circ$  axis of the container sheath. The microstructure of the metal shows a grain size of between  $10\text{-}25\mu\text{m}$ . A compact scale typically  $40\text{-}50\mu\text{m}$  thick with pits in the metal containing up to  $250\mu\text{m}$  of scale characterizes the attack on the well-protected sediment side of the container. While the macroscopic corrosion rate measurement could not precisely detect this low rate, the scale thickness can give an estimate of the corrosion rate under the assumptions that the scale represents the entire corrosion product and its density is half of that of the metal. A laminar material on the left of the photo at AB of Figure 4.12 (a) suggests an initial surface scale consistent with the assumption that the entire product formation has remained as scale. Using this argument, an estimated corrosion rate for the sediment buried side falls near 0.0025 mm/yr, assuming a linear scale growth with no induction time. This probably represents an upper limit for the general corrosion on the sediment side since a non-linear parabolic law would seem more realistic because the film appears to be protective. However, at this time it is premature to postulate a corrosion mechanism and corrosion rate. Of course, as described in previous sections, high localized corrosion completely penetrated the



sediment side as well as the sea side showing no apparent preference. This mode may in fact dominate at longer times thereby reducing the effectiveness of the container as a barrier to fission product leaching. Assuming the scale growth mode to dominate, a rather bold calculation based on a linear growth of this scale yields a time of 260 years for 50 percent loss in thickness by general corrosion, of a 1.3mm sheath buried in the sediment.

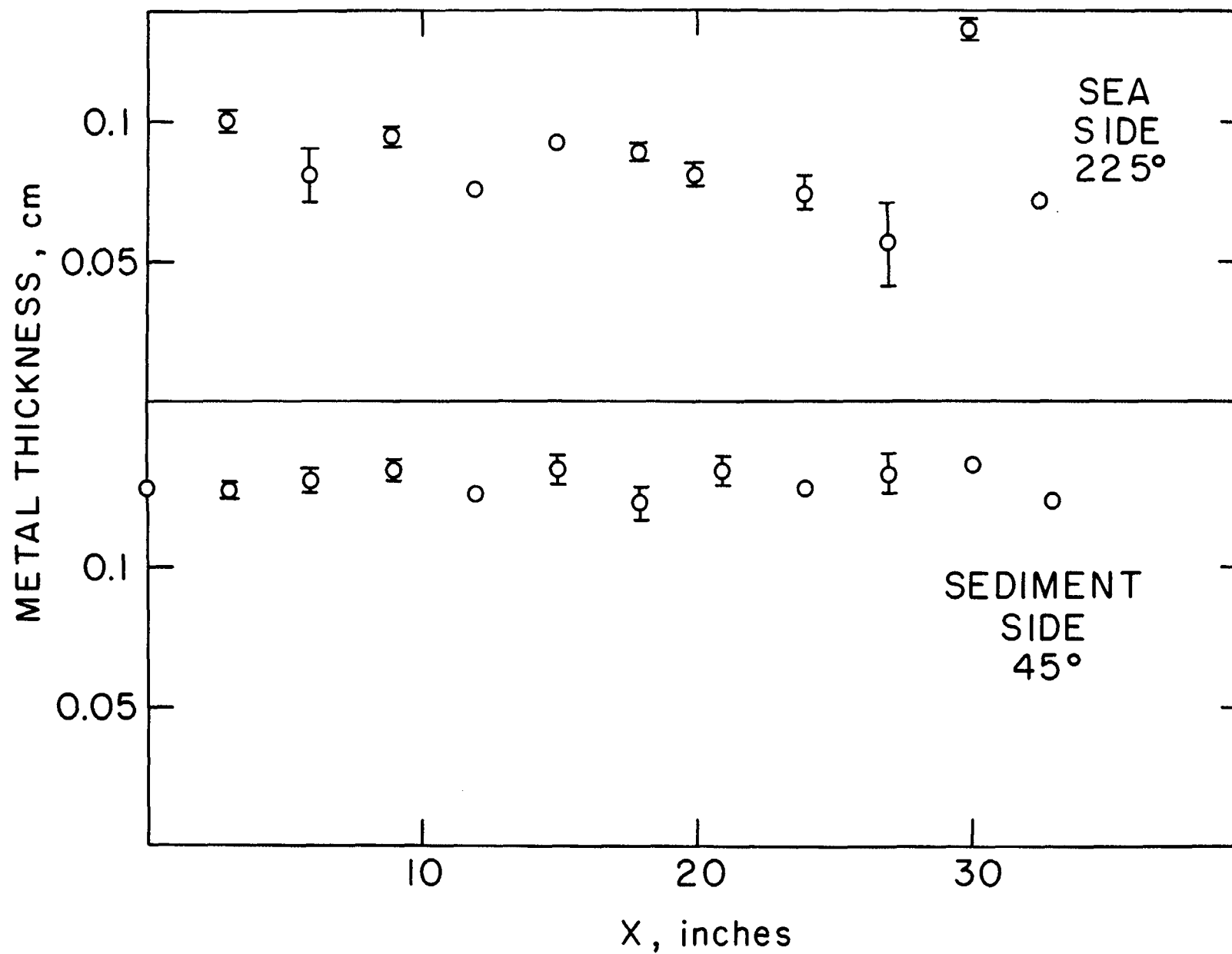


Figure 4.11 Metal Thickness as a Function of Position

TABLE 4.2  
CALCULATED CORROSION RATES

	Corrosion Rate		Ref.
	in/yr	mm/yr	
Clear Surface Waters Off Coast of Japan	0.002	0.051	(10)
Projected from Five Year Tests in Surface Waters	0.0023	0.058	(11)
Empirical Formula Zero O <sub>2</sub> Limit	0.00084	0.021	(12)
General Attack Sample I			
Sea Side	0.0013±.0002	0.033	(6)
Sediment Side	0.0019±.0002	0.048	(6)
Local Attack	>0.0026	>0.066	(6)
This Container, Sample II			
Sea Side	0.00075±.00015	0.019	
Sediment Side*	0	0	
Local Attack	>0.0021	>0.054	

\*Microscopic Examination suggests a shallow pitting and scale formation resulting in a calculated 0.0025 mm/yr average.



Figure 4.12 (b) shows a micrograph of the most severe pitting, other than the previously mentioned chime perforation, within the region of the container protected by the sediment. There is a scale growth of about  $250\mu\text{m}$  on the side of the container facing the seawater environment. Scanning Electron Microscopy (SEM) analysis of this particular sample, and the use of X-ray fluorescence showed a significant proportion of silicon in the large scale growth. On the side of this sample facing the concrete, Figure 4.12 (c), a  $20\mu\text{m}$  scale growth between the metal and dense "initial"  $\approx 5\mu\text{m}$  scale growth can be seen. Figure 4.13 gives some insight into the initiation of this secondary scale growth below the initial  $5\mu\text{m}$  scale. To the left, the initial scale can be seen breaking away from the metal. It appears that stresses on the protective initial scale can accelerate high local corrosion.

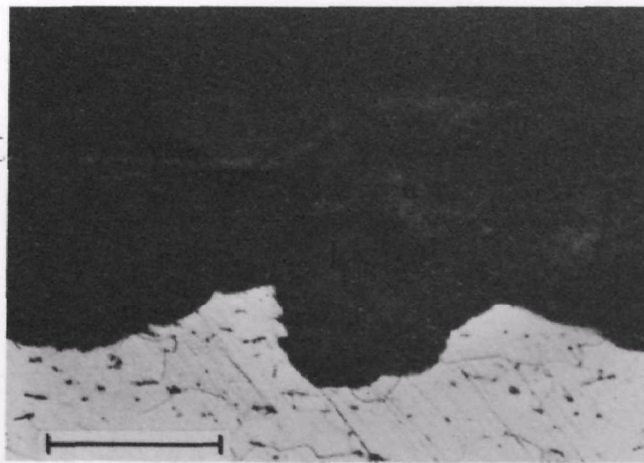
The above discussion outlines the behavior of the region on the sediment side, which appears relatively protected. Scale formation between 20 and  $50\mu\text{m}$  with some  $250\mu\text{m}$  pits characterize this region and correspond to an average  $0.0025\text{ mm/yr}$  corrosion rate. The protection probably relates to the alkaline sediment and lower oxygen activity. The overall metal loss is much less than that seen on the sea side. However, the sediment side showed the same susceptibility to high rates of localized corrosion even though the more rapid general rates appeared on the sea side of the container.

#### 4.4 CORRODED REGION ON THE SEA SIDE

A sample taken at coordinates ( $x=27^\circ$ ,  $\theta=225^\circ$ ) represents the "worst case" general corrosion (here general corrosion is distinguished from the high local attack experienced by the rim and chimes). Figure 4.14 shows the scale formed on the sea side of this sample. In contrast to that of the more protected region, Figure 4.15 shows that this surface exhibits a very porous structure with many cracks in the scale extending entirely through the metal surface.

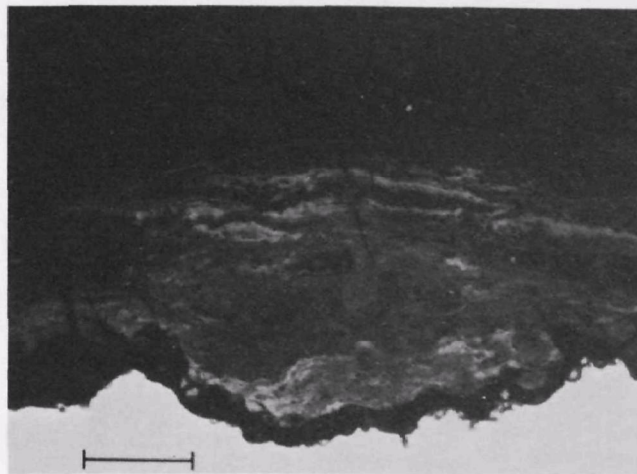
As shown in Figure 4.16, the concrete side of this sample shows a more compact scale formation. Significantly a thick  $20\mu\text{m}$  to  $50\mu\text{m}$  oxide (EF) forms under the initially existent lamina, oxide (CD) and "coating" (BC). The identification of these layers are based on X-ray fluorescence (XRF) evidence provided in Figure 4.17. Here the scales (CD and EF) are shown to contain iron and are assumed to be oxides of iron. Area DE represents a void resulting from delamination. Area AB contains aluminum and is, therefore, part of the concrete waste form, while region BC shows neither iron nor aluminum. Section BC probably represents the remnants of a coating, although no evidence of this "coating" has been found on the remainder of the vessel even though repeated searches were made with the aid of the Brookhaven National Laboratory metallography laboratory. The  $5\mu\text{m}$  thick scale, CD, remains on much of the well-protected portions of the container.

A—  
B—  
a.



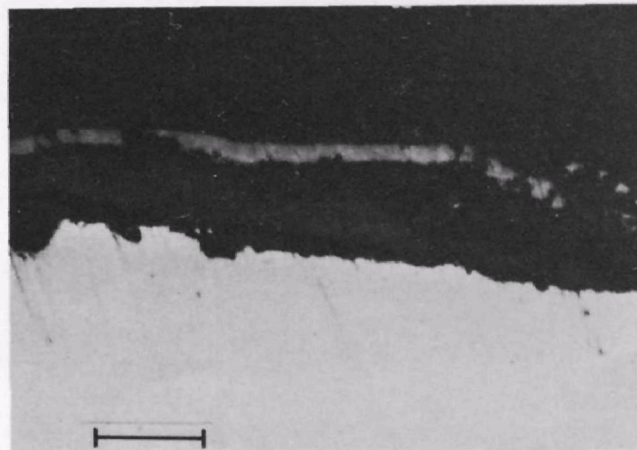
Typical Outer Scale

b.



Worst Case Outer Scale

c.



Concrete Side Scale

Figure 4.12 Optical Micrograph of Well Protected Specimens Taken from Positions ( $x = 9$  inches,  $\theta = 45$ ), ( $x = 15$  inches,  $\theta = 45$ ) respectively

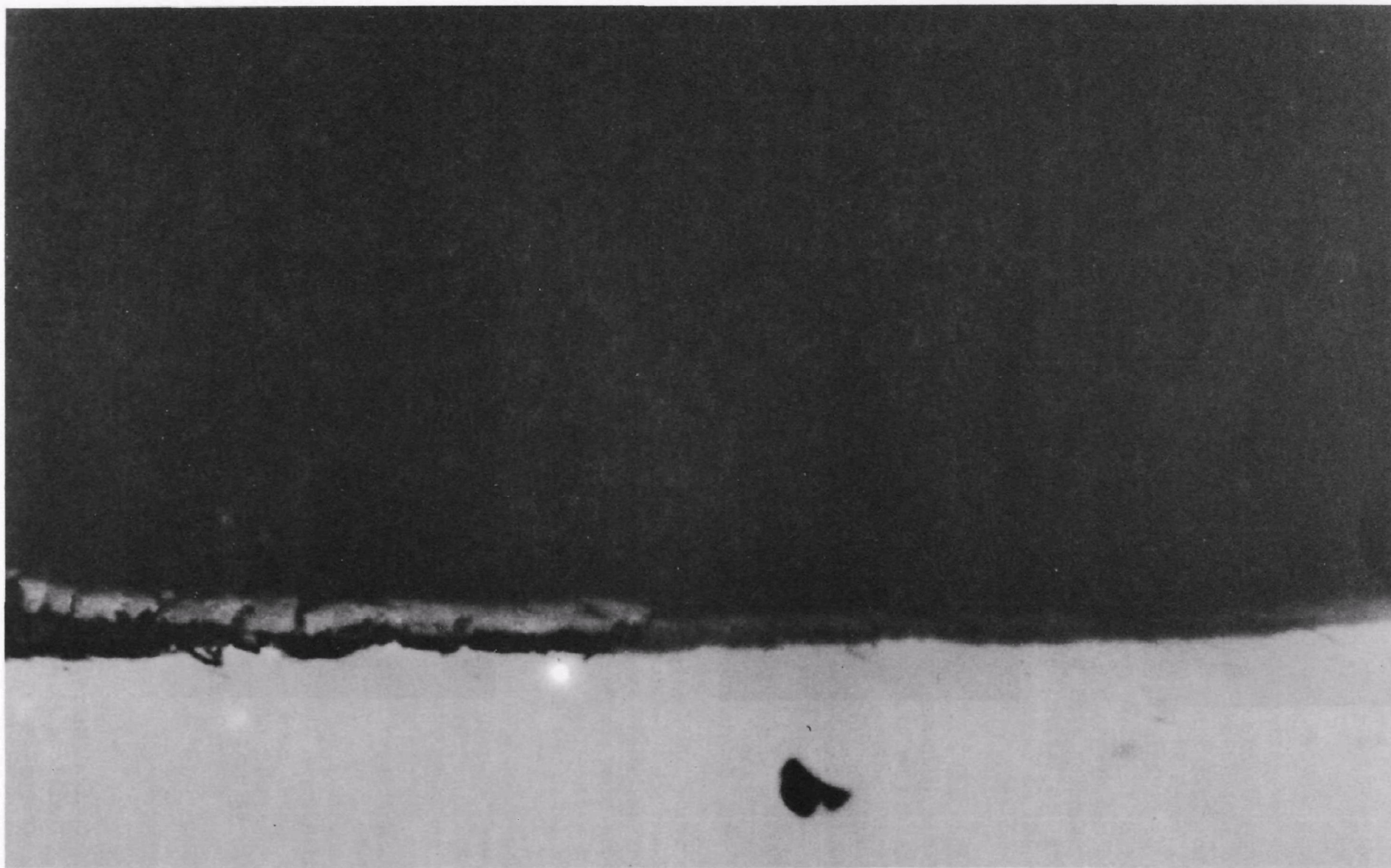


Figure 4.13 Initiation of Corrosion on the Sediment Side of the Container  
( $x=12$  inches,  $\theta = 46^\circ$ )

40  $\mu$



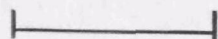
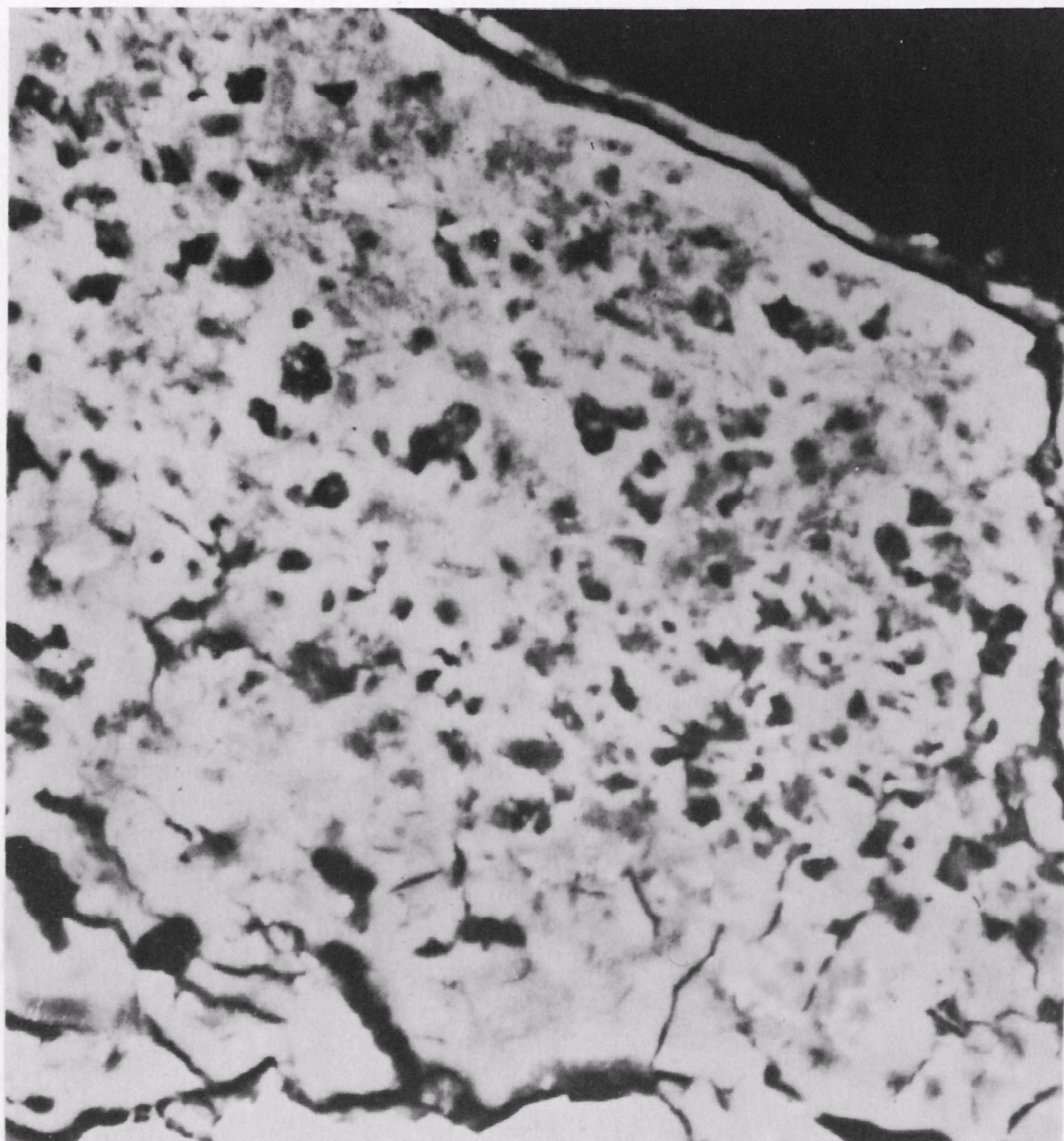


Figure 4.14 Rapid General Corrosion on Sample Taken from X=27 inches,  $\theta = 225^\circ$



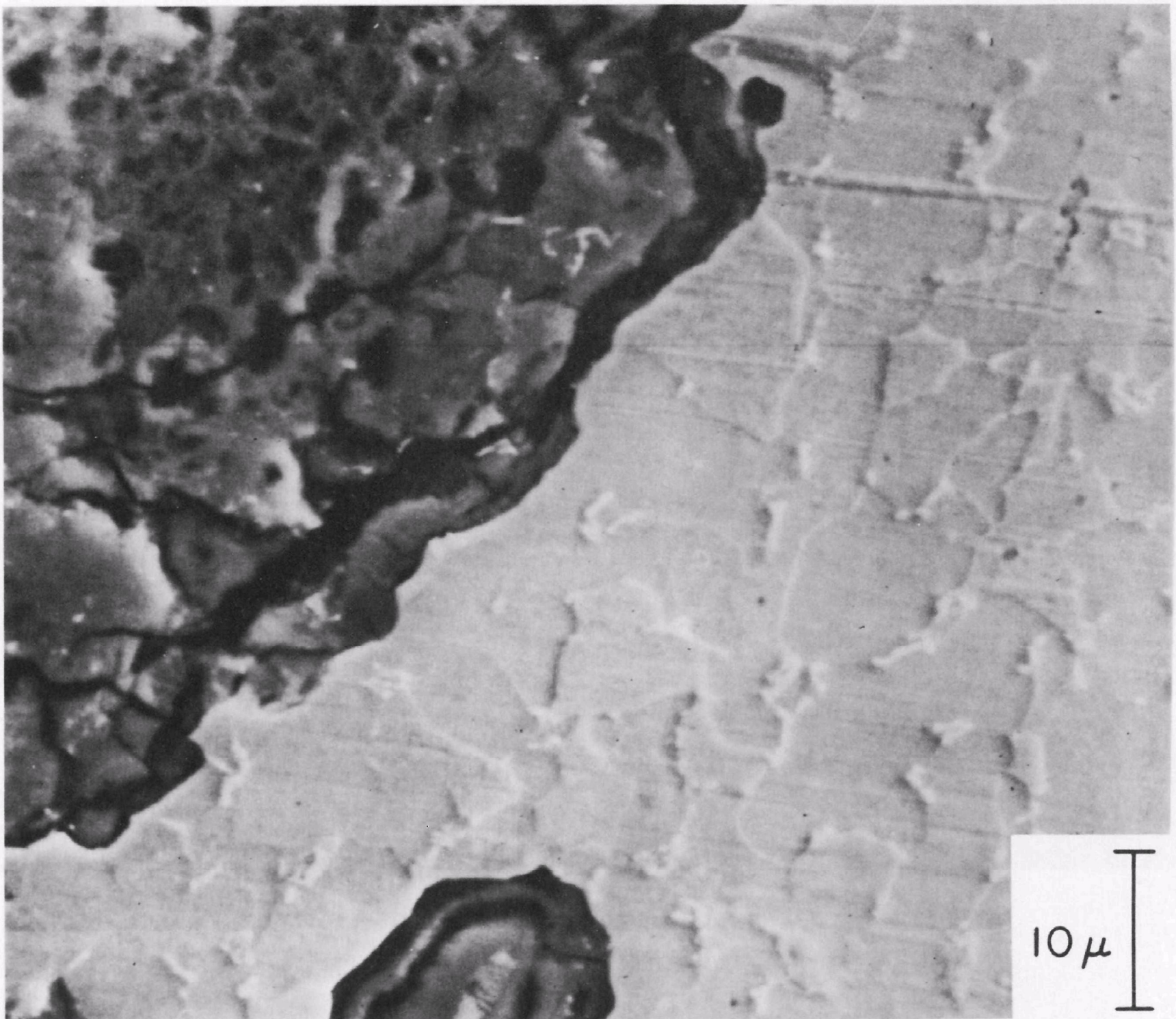


Figure 4.15 Metal to Scale Interface of Sample Taken From x=27 inches,  $\theta = 225^\circ$



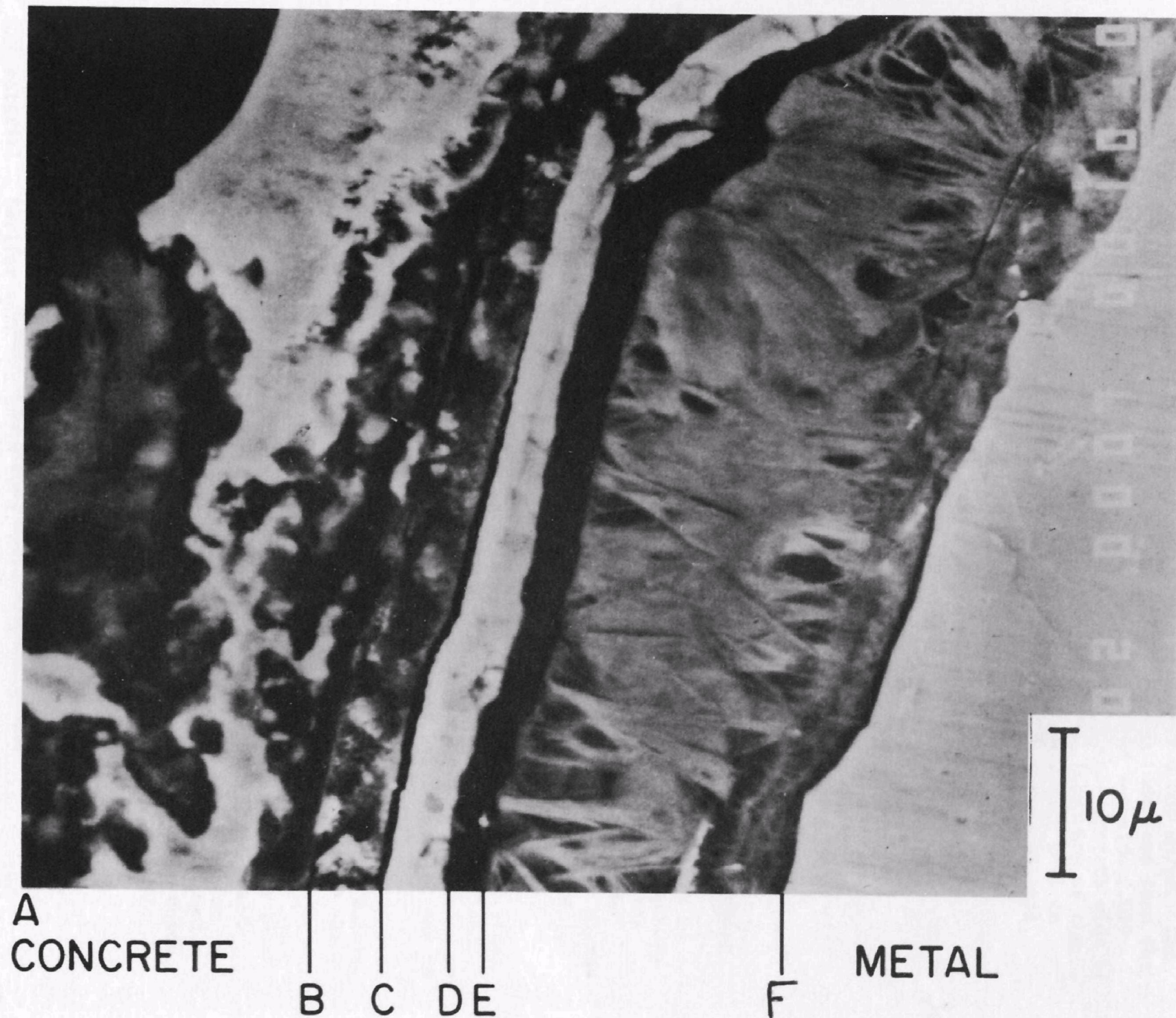
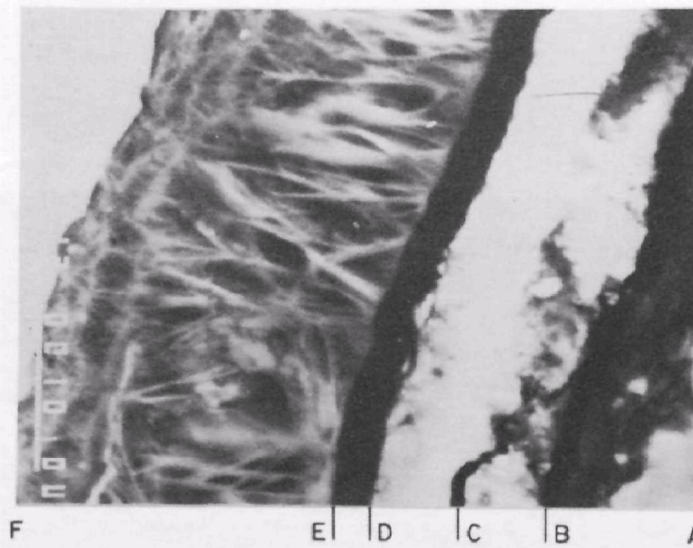
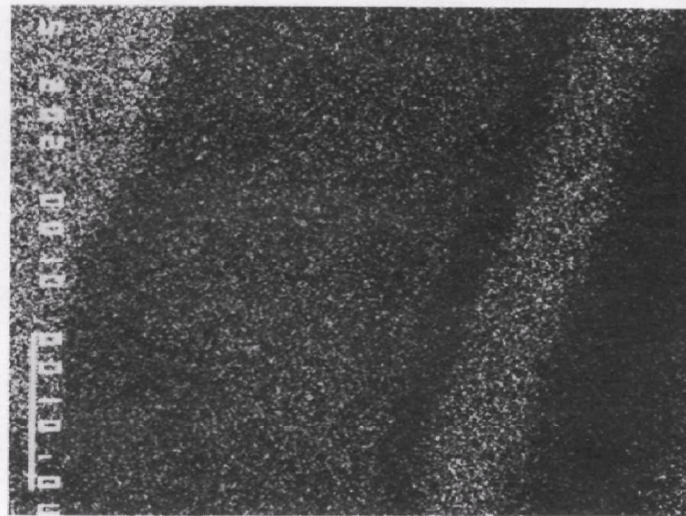


Figure 4.16 Corrosion Scale of Sample (Concrete Side) Taken From x=27 inches,  $\theta = 225^\circ$



a. Scanning electron  
micrograph  
(SEM)



b. x-ray fluorescence  
map of iron



c. x-ray fluorescence  
map of aluminum

Figure 4.17 Solid Phase Analysis of Concrete Side Lamina of Sample Taken from  $x=27$  inches,  $\theta = 225^\circ$



The inner scale represents a metal corrosion rate of about 0.001 mm/yr, for the concrete side of the sample. This is an order of magnitude less than the measured average of the total corrosion rate on the exposed sea side (.019 mm/yr). However, any detrimental effects of corrosion on the concrete side of the container should be considered since it impacts on the longevity of the container. For this reason, the following calculations have been made to assess the significance of the growth of the oxide film on the mechanical integrity of the package.

Referring to Figure 4.18, an oxide scale of thickness  $\delta x$  will produce a fractional radial strain  $\delta r/R$ , expressed as:

$$\epsilon = \frac{\delta r}{R} = \left(1 - \frac{\rho_{\text{oxide}}}{\rho_{\text{metal}}}\right) \frac{\delta x}{R}$$

where:  $\rho_{\text{oxide}}$  = oxide density     $R$  = radius of the container  
 $\rho_{\text{metal}}$  = metal density     $\delta r$  = change in radius caused by corrosion

Using a density ratio of 0.5,  $\epsilon = 8.7 \times 10^{-5}$  for 100  $\mu\text{m}$  oxide growth. This is equal to the circumferential strain on the metal. An assumed elastic modulus of  $30 \times 10^6$  psi [13] for the material results in a calculated stress on the metal of  $2.6 \times 10^3$  psi corresponding to an excess pressure of 24 psi on the concrete. These values correspond to nonsusceptible regions for either stress corrosion cracking (SCC) of the carbon steel [14,15] or breakdown in the concrete [6] and hence are not significant.

Table 4.3 shows an analysis of the trace elements present in the carbon steel sheath of the waste package. The composition or structure of the material does not differ significantly from the previous container [6]. Differences in apparent corrosion rates between the two containers must, therefore, be due to the respective environments.

The scrapings primarily contain iron compounds. Traces of other heavy metals, as shown in Table 4.4, have also been found and probably originate from the environment.

Table 4.5 shows that the scrapings are comprised primarily of the  $\alpha$  and  $\gamma$  hydrated  $\text{Fe}_2\text{O}_3$  species. The most prevalent form,  $\alpha$  - hydrated ferric oxide ( $\gamma\text{-FeOOH}$ ) results from the aging of the  $\gamma$  form in the neutral to alkaline water [16]. The predominance of the  $\alpha$  form of the hydrated iron oxide product suggests a slowing of the corrosion process from the initial rates which would result in the predominance of the  $\gamma\text{-FeOOH}$  product.

In general, little knowledge exists about precise mechanisms governing corrosion in deepsea environments for long time periods. Typically, metal loss will be a nonlinear function of time, temperature, and activity of certain reactive, catalytic or inhibiting elements in the environment and material. Earlier work has shown metal corrosion of well characterized samples to be linear in time, temperature and oxygen concentration for low

temperatures and time  $\leq 5$  years [6]. This must be considered to be a first approximation. Longer term analysis requires a more detailed description of the mechanisms contributing to the corrosion of the sheath in order to obtain the higher order time and temperature terms for the rate equation required for the time periods  $> 5$  years.

Furthermore, use of accelerated tests to specify mechanisms or extrapolate rates can produce misleading results for metal-concrete systems [17]. With these considerations in mind, the "corrosion rates" specified throughout this report are calculated rates based on assumptions of constant rate with no induction time. These are questionable assumptions, but their use for estimating rates are justified on the grounds that the estimated rates provide a means of comparison. For example, the general rate of corrosion on the sea side of this container exceeds that of the previously examined sample taken from the Atlantic Ocean 2800 meter site [6].



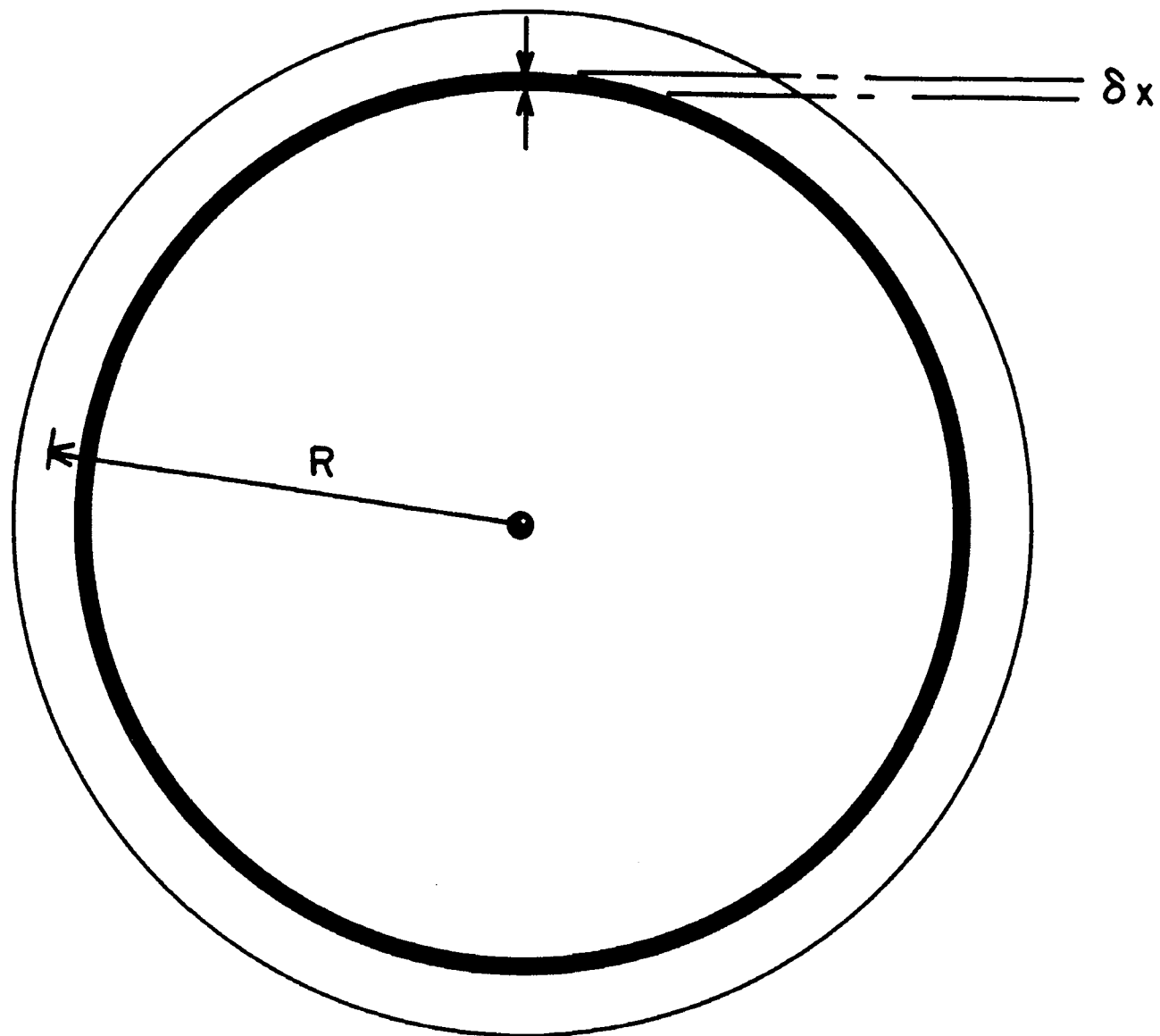


Figure 4.18 Schematic of Container with Scale Growth

TABLE 4.3

TRACE ELEMENT ANALYSES OF CONTAINER MATERIAL

<u>ELEMENT</u>	<u>WEIGHT PERCENT</u>
C	0.10
Mn	0.36
P	0.007
S	0.030
Si	ND <0.02
Ni	ND <0.02
Cr	ND <0.02
Mo	ND <0.02
Cu	0.1



TABLE 4.4

X-RAY FLUORESCENCE ANALYSIS OF TRACE COMPONENTS IN SCRAPINGS

<u>Sample</u>	<u>Position</u>		<u>Trace Elements</u>
	X(cm.)	$\theta$ (degrees)	
II-1	88.5	0 - 270	Cu, Ti, V, Mn ~30 ppm Zn, Pb, ~10ppm
II-4	23	163	Ti ~30 ppm >Zn
II-5	31	180	Small Cu, Zn
II-7	41	25	Si, Ci, K, Ca ~50 ppm, Ti, Cr, Mn 10-30 ppm

TABLE 4.5

X-RAY DIFFRACTION ANALYSIS OF MAJOR IRON OXIDE COMPONENT

<u>Sample</u>	<u>Position</u>		<u>Corrosion Products</u>
	X(cm.), $\theta$ (degrees)		
II-1	88.5	0 -270	$\alpha$ - FeOOH, $\gamma$ - FeOOH
II-4	23	165	$\alpha$ - FeOOH
II-5	32	180	$\alpha$ - FeOOH
II-6	86	0 - 270	$\alpha$ - FeOOH



## 5. CONCLUSIONS

The following summarizes the conclusions of this study:

- (a) The concrete waste form maintained a high degree of integrity during the time (21-23 years) that it was exposed to the ocean environment. This can be attested to by the condition of the cardboard box within the waste form and the resistance of the concrete to hydrostatic implosion, considering a void cavity of approximately 1,200 cubic inches.
- (b) The measured compressive strength of the concrete cores is in a much higher range than that found at the Atlantic 2800-meter disposal site [6]. The degree of uniformity in the strength values obtained from cores taken throughout the waste form are indicative of its durability in the ocean environment.
- (c) The sediment apparently inhibits general corrosion. The scale thickness, observed for the sediment side of the container, corresponds to an estimated 0.0025 mm/yr constant corrosion rate with no induction time or a 260-year time for 50 percent reduction in thickness of a 1.3mm sheath.
- (d) The metal loss on the sea side of the container corresponds to a constant corrosion rate of 0.019 mm/yr or a 34-year time required for 50 percent reduction in thickness of a 1.3mm sheath.
- (e) High rates of localized attack perforated regions of cold work, e.g., rims and chimes. More perforation occurred on the sea side. This effect could result from (1) higher elementary processes on cold work metal surfaces, (2) higher stresses produced in protective scales or coatings as a result of underside film growth, or (3) a combination of these effects. Further investigation is recommended in order that the best ameliorative design can be made for future use.
- (f) The metal loss results primarily from the sea side formation of a porous loosely adhering scale and not from concrete side corrosion.
- (g) The corrosion on the concrete side typically formed 50 $\mu$ m to 100 $\mu$ m scale with some 250  $\mu$ m pits in the 24 years. The calculated mechanical effect this has on the concrete or metal is negligible even when possible alkaline stress crack corrosion is considered.

## REFERENCES

1. "A Survey of the Farallon Islands 500-Fathom Radioactive Waste Disposal Site-Operations Report," U.S. Environmental Protection Agency, Report No. ORP-75-1, Washington, DC (1975).
2. Joseph, A.B., "A Summary to December 1956 of the U.S. Sea Disposal Operations," WASH 734, U.S. Atomic Energy Commission, Washington, DC (1957).
3. Dyer, R.S., Environmental Surveys of Two Deep Sea Radioactive Waste Disposal Sites Using Submersibles," In: Management of Radioactive Wastes from the Nuclear Cycle, Vol. II, IAEA, Vienna, Austria (1976).
4. Interstate Electronics Corporation, "A Survey of the Farallon Islands 500-Fathom Radioactive Waste Disposal Site," IEC Report 4460C1648, prepared for the U.S. Environmental Protection Agency Office of Radiation Programs and Office of Water Program Operations by IEC, Anaheim, CA, December 1975.
5. Dayal, R., I.W. Duedall, M. Fuhrmann, and M.G. Heaton, "Sediment and Water Column Properties at the Farallon Islands Radioactive Waste Dumpsite," Draft Report, April 1979, Submitted to the Office of Radiation Programs, U.S. Environmental Protection Agency, Washington, DC.
6. Colombo, P., R. Neilson and M. Kendig, "Analysis and Evaluation of a Radioactive Waste Package Retrieved from the Atlantic 2800 Meter Disposal Site," EPA 520/1-82-009, BNL 51102, Office of Radiation Programs, U.S. Environmental Protection Agency, Washington, DC, May 1982.
7. Uhlig, H.H., Corrosion and Corrosion Control, second edition, John Wiley, P. 92, (1971).
8. Miller, J.D.A., Microbial Aspects of Metallurgy, Editor, American Elsevier, (1970).
9. National Association of Corrosion Engineers, Technical Practices Committee, "Recommended Practice, Collection and Identification of Corrosion Products," NACE Standard RP-01-73, February 1973, Houston, Texas.
10. Kakehi, T. and H. Yoshino, "Corrosion of Steel in Polluted Sea Waters," Proc. 5th Int. Cong. on Met Corrosion, 1972, NACE (1974), p. 76.
11. Tamada, A., M. Tammura and G. Tennyoy, "Corrosion Behavior of Low Alloy Steels in Sea Water," Ibid, p. 786.

12. Reinhart, F.M. and J. R. Jenkins, "The Relationship Between the Concentration of Oxygen in Sea Water and Corrosion of Metals," Proc. 3rd Congr. on Marine Corrosion and Fouling, p. 562 et. eq. 1972.
13. American Society for Metals, Metals Handbook, p. 427, Vol. 1, 8th Edition, Metal's Park, Ohio (1975).
14. Reinoehl, J.E. and W.E. Berry, Corrosion, 28 (4), 151 (1972).
15. Humphries, M.J. and R.N. Parkins, Corrosion Sciences, 7, 474 (1967).
16. Misawa, T., K. Hashimoto and S. Shumodiara, "The Mechanism of Formation of Iron Oxide and Oxyhydroxides in Aqueous Solutions at Room Temperature," Corrosion Science, 14, 131 (1974).
17. Tuutti, K., "Cracks and Corrosion. The Corrosion of steel in Concrete--the Effects of Cracks in the Concrete Cover." CBI Forsk. 1978 (6), referenced in Chem. Abstracts.



<b>TECHNICAL REPORT DATA</b> <i>(Please read Instructions on the reverse before completing)</i>		
1. REPORT NO. EPA 520/1-90-014	2.	3. RECIPIENT'S ACCESSION NO.
4. TITLE AND SUBTITLE Analysis and Evaluation of a Radioactive Waste Package Retrieved from the Farallon Islands 900-meter Disposal Site	5. REPORT DATE September 1990	6. PERFORMING ORGANIZATION CODE
7. AUTHOR(S) P. Colombo and M.W. Kendig, Brookhaven National Laboratory	8. PERFORMING ORGANIZATION REPORT NO.	
9. PERFORMING ORGANIZATION NAME AND ADDRESS Brookhaven National Laboratory Nuclear Waste Research Group Department of Nuclear Energy Upton, New York 11973	10. PROGRAM ELEMENT NO.	11. CONTRACT/GRANT NO. Interagency Agreement No. EPA-IAG-D6-0166
12. SPONSORING AGENCY NAME AND ADDRESS U.S. Environmental Protection Agency Office of Radiation Programs 401 M Street, SW Washington, DC 20460	13. TYPE OF REPORT AND PERIOD COVERED Final	14. SPONSORING AGENCY CODE ANR-461
15. SUPPLEMENTARY NOTES		
16. ABSTRACT  <p>In October of 1977, a 55-gallon low-level radioactive waste (LLW) package was retrieved from the Farallon Islands 900-meter disposal site located 40 miles west of San Francisco, California, at coordinates 37°38'N and 123°08'W. This was the second recovery of a LLW package from an ocean disposal site and was conducted by the EPA Office of Radiation Programs. The waste package was transported to Brookhaven National Laboratory where container corrosion and matrix analysis studies were performed. This report presents the final results of the laboratory analyses and contains detailed photographic documentation of the recovery operation and condition of the waste package.</p>		
17. KEY WORDS AND DOCUMENT ANALYSIS		
a. DESCRIPTORS	b. IDENTIFIERS/OPEN ENDED TERMS	c. COSATI Field, Group
1. radioactive waste disposal 2. radioactive waste packaging 3. marine corrosion 4. ocean dumping/sea disposal		
18. DISTRIBUTION STATEMENT Release Unlimited	19. SECURITY CLASS (This Report) Unclassified	21. NO. OF PAGES 78
	20. SECURITY CLASS (This page) Unclassified	22. PRICE



United States  
Environmental Protection  
Agency  
(ANR-459)  
Washington, DC 20460

Official Business  
Penalty for Private Use  
\$300